A hydrogeomorphological index of heavy-tailed flood behavior

Hsing-Jui Wang[1], Ralf Merz[2], Soohyun Yang[3], and Stefano Basso[4]

[1]Helmholtz-Centre for Environmental Research UFZ
[2]Helmholtz Centre for Environmental Research (UFZ)
[3]Helmholtz Centre for Environmental Research-UFZ
[4]Helmholtz Centre for Environmental Research

December 22, 2022

Abstract

Floods are often disastrous due to underestimation of the magnitude of rare events. When the occurrence of floods follows a heavy-tailed distribution the chance of extreme events is sizable. However, identifying heavy-tailed flood behavior is challenging because of limited data records and the lack of physical support for currently used indices. We address these issues by deriving a new index of heavy-tailed flood behavior from a physically-based description of streamflow dynamics. The proposed index, which is embodied by the hydrograph recession exponent, enables inferring heavy-tailed flood behavior from daily flow records. We test the index in a large set of case studies across Germany. Results show its ability to identify cases with either heavy- or nonheavy-tailed flood behavior, and to evaluate the tail heaviness. Remarkably, the results are robust also for decreasing the lengths of data records. The new index thus allows for assessing flood hazards from commonly available data.

A hydrogeomorphological index of heavy-tailed flood behavior

H. -J. Wang[1], R. Merz[1,2], S. Yang[3], and S. Basso[1,4]

[1]Department of Catchment Hydrology, Helmholtz Centre for Environmental Research – UFZ, Halle (Saale), Germany,

[2]Institute of Geosciences and Geography, Martin-Luther University Halle-Wittenberg, Halle (Saale), Germany,

[3]Department of Aquatic Ecosystem Analysis, Helmholtz Centre for Environmental Research – UFZ, Magdeburg, Germany

[4]Norwegian Institute for Water Research (NIVA), Oslo, Norway

Corresponding author: Hsing-Jui Wang (hsing-jui.wang@ufz.de)

Key Points:

- The hydrograph recession exponent is identified as an index of heavy-tailed flood behavior.
- The proposed index enables robust identification of heavy-tailed flood behavior in a large set of case studies and from short data records.
- Unlike other frequently used metrics, the proposed index infers heavy-tailed flood behaviors from commonly observed discharge dynamics.

Abstract

Floods are often disastrous due to underestimation of the magnitude of rare events. When the occurrence of floods follows a heavy-tailed distribution the chance of extreme events is sizable. However, identifying heavy-tailed flood behavior is challenging because of limited data records and the lack of physical support for currently used indices. We address these issues by deriving a new index of heavy-tailed flood behavior from a physically-based description of streamflow dynamics. The proposed index, which is embodied by the hydrograph recession exponent, enables inferring heavy-tailed flood behavior from daily flow records. We test the index in a large set of case studies across Germany. Results show its ability to identify cases with either heavy- or nonheavy-tailed flood behavior, and to evaluate the tail heaviness. Remarkably, the results are robust also for decreasing the lengths of data records. The new index thus allows for assessing flood hazards from commonly available data.

Plain Language Summary

High flow events often cause severe damages when they occur unexpectedly, i.e., more often and with larger magnitudes than suggested by historical observations. This is usually the case with frequency distributions of floods which are heavy-tailed. However, a proper assessment of the tail behavior solely based on limited data records is difficult and might lead to an erroneous estimation of the underlying hazard. We start by analyzing runoff generation processes and find that the hydrograph recession is a proper descriptor of the emergence of heavy-tailed behavior. Our findings show that the new proposed index allows for (1) detecting cases with heavy-tailed behavior, (2) comparing severity across cases, and (3) displaying robust results also with short data records. These results address the main limitations of currently used metrics (which often require long records and lack physical meaning) and provide information on the characteristic flood hazard of river basins.

1 Introduction

Floods remain the leading natural hazards worldwide, which directly threaten at least one-fifth of people's livelihoods (McDermott, 2022; Rentschler et al., 2022) and have caused enormous and increasing economic losses (Bevere & Remondi, 2022) in recent years. Floods are often disastrous because they occur unexpectedly (i.e., underestimated by water resources managers as well as residents) (Else, 2021; Merz et al., 2021), commonly due to poor estimates of the magnitude of rare events obtained from available observations. A number of studies in natural and anthropogenic phenomena use heavy-tailed distributions to describe the extreme behavior of variables (e.g., Katz, 2002; Kondor et al., 2014; Malamud, 2004; Sartori & Schiavo, 2015; Wang et al., 2022) because it indicates a sizable chance of the occurrence of extreme value. We can better assess the flood hazards if we may know that floods follow a heavy-tailed distribution, i.e., robustly identify the heavy-tailed flood behavior (Merz et al., 2022).

A variable distribution's tail heaviness is traditionally estimated graphically or mathematically, while both have their limitations. In general, graphical methods such as log-log plots (Beirlant et al., 2004), generalized Hill ratio plots (Resnick, 2007; El Adlouni et al., 2008), and mean excess functions (Embrechts et al., 1997; Nerantzaki & Papalexiou, 2019) have less objectivity and efficiency (Cooke et al., 2014). Mathematical methods provide more objective insights into the estimation of tail behavior. The shape parameters of Generalized Extreme Value (GEV) distributions quantify the tail behavior by fitting the parameters of an underlying distribution on limited records of maxima (Morrison & Smith, 2002; Villarini & Smith, 2010; Papalexiou et al., 2013), and a group of non-parametric metrics evaluates the spread of data (e.g., upper tail ratio (Lu et al., 2017; Smith et al., 2018; Villarini et al., 2011; Wang et al., 2022), Gini index (Eliazar & Sokolov, 2010; Rajah et al., 2014), and obesity index (Cooke & Nieboer, 2011; Sartori & Schiavo, 2015)). These methods often require long records to obtain reliable estimates (Papalexiou & Koutsoyiannis, 2013). This is a challenge globally and even more challenging when it comes to analyzing maxima (which is indeed the key to assessing hazards of extreme floods). The bias caused by the data size restricts the comparability across sites with different record lengths (Wietzke et al., 2020). In addition, the correctness of the estimation of tail heaviness is influenced by the underlying physical processes of the case studies (Merz et al., 2022). However, to the best of our knowledge, physical processes are absent from these frequently used metrics. It is preferable to have a new index that can robustly estimate with data in different lengths (Bernardara et al., 2008; Merz & Blöschl, 2009) and is based on the physical processes that favor the heavy-tailed behavior of flood distributions.

We propose a new index of heavy-tailed flood behavior, which can be estimated by common discharge dynamics. Unlike fitting a statistical distribution to observed series of maxima (which may not clearly exhibit heavy-tailed behavior due to data scarcity), the index infers the tail heaviness of floods by examining the intrinsic dynamics of the hydrological system. Reliable identification of heavy tails by the proposed index is tested in datasets with decreasing lengths in a great number of case studies with various climate and physiographic features. We leverage common discharge dynamics to facilitate flood peril assessment and demonstrate its usefulness in areas with limited records.

2 Identifying tail behavior from hydrological dynamics

We describe key hydrologic dynamics occurring at the catchment scale and the resulting probability distributions of streamflow and floods by means of the PHysically-based Extreme Value (PHEV) distribution of river flows (Basso et al., 2021). This framework is grounded on a well-established mathematical description of precipitation, soil moisture, and runoff generation in river basins (Laio et al., 2001; Porporato et al., 2004; Botter et al., 2007b, 2009). Rainfall is described as a marked Poisson process with frequency $\lambda_p [\mathrm{T}^{-1}]$ and exponentially distributed depths with average α [L]. Soil moisture increases due to rainfall infiltration and decreases due to evapotranspiration. The latter is represented by a linear function of soil moisture between the wilting point and an upper critical value expressing the water holding capacity of the root zone. Runoff pulses occur with frequency $\lambda < \lambda_p$ when the soil moisture exceeds the critical value. These pulses replenish single catchment storage, which drains according to a nonlinear storage-discharge relation. The related hydrograph recession is described via a power law function with exponent $a\,[-]$ and coefficient $K\,[\mathrm{L}^{1-a}/\mathrm{T}^{2-a}]$ (Brutsaert & Nieber, 1977), which allows for mimicking the joint effect of different flow components (Basso et al., 2015). Such a description of runoff generation and streamflow dynamics was successfully tested in a variety of hydro-climatic and physiographic conditions (Arai et al., 2020; Botter et al., 2007a; Botter et al., 2010; Ceola et al., 2010; Doulatyari et al., 2015; Mejía et al., 2014; Müller et al., 2014; Müller et al., 2021; Pumo et al., 2014; Santos et al., 2018; Schaefli et al., 2013).

PHEV provides a set of consistent expressions for the probability distributions of daily streamflow, ordinary peak flows (i.e., local flow peaks occurring as a result of streamflow-producing rainfall events; Zorzetto et al., 2016), and floods (i.e., flow maxima in a certain timeframe; Basso et al., 2021). For example, the probability distribution of daily streamflow q can be expressed as (Botter et al., 2009):

$$p(q) = C_1 \cdot q^{-a} \left(e^{\frac{-1}{\alpha K(2-a)} \cdot q^{2-a}} \right) \left(e^{\frac{\lambda}{K(1-a)} \cdot q^{1-a}} \right) \tag{1}$$

where C_1 is a normalization constant.

Taking the limit of Equation (1) for $q \to +\infty$ gives indications of the tail behavior of the flow distribution (Basso et al., 2015). This is determined by the three terms in the equation, namely, one power law and two exponential functions, which behave differently depending on the value of the hydrograph recession exponent a (Equation 2; notice that $a > 1$ in most natural river basins; Tashie et al., 2020a).

$$\lim_{q \to +\infty} p(q) = \lim_{q \to +\infty} \left\{ C_1 \cdot \overbrace{\underbrace{q^{-a}}_{\mapsto 0}}^{\mapsto 0} \overbrace{\underbrace{\left(e^{\frac{-1}{\alpha K(2-a)} \cdot q^{2-a}} \right)}_{\mapsto e^0 = 1}}^{\mapsto 0} \overbrace{\underbrace{\left(e^{\frac{\lambda}{K(1-a)} \cdot q^{1-a}} \right)}_{\mapsto e^0 = 1}}^{\mapsto e^0 = 1} \right\} \quad \begin{matrix} \text{for } 1 < a < 2 \\ \\ \text{for } a > 2 \end{matrix} \tag{2}$$

When $1 < a < 2$, the last term on the right-hand side converges to a constant value of one as q increases, thereby no more influence on how the distribution decreases toward zero. The first two terms instead decrease toward zero, affecting how the probability decreases for increasing values of q. The tail behavior is in this case determined by both a power law and an exponential functions, indicating that the probability decreases faster than an exponential but slower than a power law. When $a > 2$, both the exponential terms converge to a constant value of one as q increases, and thus no more influence on how the probability decreases toward zero. In this case the tail of the distribution is solely determined by the power law function. Despite being aware that several definitions of heavy-tailed distribution exist (El Adlouni et al., 2008; Vázquez et al., 2006), in the remaining of the manuscript we refer to heavy-tailed behavior for the case of distributions which exhibit a power law tail (i.e., the cases with a > 2). We thus aim to distinguish them from cases which display a lighter tail because of the simultaneous effect of exponential decay (i.e., the cases with 1 < a < 2).

From the above derivations, the hydrograph recession exponent emerges as a key index of the tail behavior of streamflow distributions, which shall be heavy-tailed for values of $a > 2$. The same analysis applies to infer the tail behavior of the probability distributions of ordinary peak flows (Botter et al., 2009) and floods (Basso et al., 2016) (see supporting information Text S1). Remarkably, we find that the same critical value of the recession exponent indicates the emergence of heavy-tailed behavior also in peak flow and flood distributions. We therefore propose the hydrograph recession exponent a as an index for identifying heavy-tailed flood behavior, and test its capability to correctly predict such behavior in Section 4.

Recent studies showed that the hydrograph recession exponent is a convincing descriptor of the geomorphological signature of drainage areas (Biswal & Marani, 2010, 2014; Biswal & Kumar, 2014; Ghosh et al., 2016; Mutzner et al., 2013). The river network structure primarily defines how the geometry of saturated (Mutzner et al., 2013) and unsaturated areas (Biswal & Marani, 2010) of a river basin change over the draining process, which essentially determines the streamflow dynamics at the outlet. Despite being aware of the influences of seasonal climate (Jachens et al., 2020; Tashie et al., 2019), the geomorphological structure of the contributing river network has been demonstrated as the major determinator of the hydrograph recession exponent (Biswal & Kumar, 2014; Ghosh et al., 2016). We thus refer to the hydrograph recession exponent for a hydrogeomorphological index of heavy-tailed flood behavior.

3 Data and parameter estimation

To test the proposed hydrogeomorphological index of heavy-tailed flood behavior (i.e., the hydrograph recession exponent a), we use streamflow records with daily time resolution of 98 gauges across Germany (Figure S1). The analyzed river basins encompass a variety of climate and physiographic settings (Tarasova et al., 2020), while not being heavily affected by anthropogenic flow regulation and snow dynamics across seasons. Their areas range from 110 to 23,843 km^2 with a median value of 1,195 km^2. The minimum, median, and maximum lengths of the streamflow records are 35, 58, and 63 years (inbetween 1951 – 2013). We perform all analyses on a seasonal basis (winter: December–February, spring: March–May, summer: June–August, fall: September–November) to account for the seasonality of the hydrograph recessions and flood distributions (Durrans et al., 2003; Tashie et al., 2020b). This results in an overall number of 386 case studies used in our study.

We estimated a as the median value of the exponents of power law functions fitted to $dq/dt - q$ pairs of each hydrograph recession observed in the daily flow series (Jachens et al., 2020; Biswal, 2021). Notice that the proposed indicator of heavy-tailed flood behavior is thus estimated based on commonly available daily discharge observations.

The identification of case studies with either heavy- or nonheavy-tailed behavior resulting from the proposed index must be evaluated against a suitable benchmark. This is obtained by means of a state-of-the-art approach to fit power law functions to empirical distributions and evaluate their plausibility for the analyzed data (Clauset et al., 2009). The fitted exponent is here noted as b. We analyze three types of empirical data, namely daily streamflow, ordinary peaks, and monthly maxima (Fischer & Schumann, 2016; Malamud & Turcotte, 2006), and obtain estimates of the fitted exponent b for each case. These results will be used to validate the capabilities of the proposed hydrogeomorphological index to infer heavy-tailed flood behavior from the analysis of hydrograph recessions.

4 Results and discussion

We examine if power law distributions fitted to the empirical distributions of daily streamflow, ordinary peaks, and monthly maxima well describe the observed data for the case studies identified as having heavy-tailed behavior (i.e., a > 2) according to the hydrogeomorphological index (Figure 1). First, we identify the case studies with either heavy- (a > 2; red) or nonheavy (a < 2; green) -tailed behavior based on the hydrogeomorphological index. Then, we use the Kolmogorov-Smirnov (KS) statistic κ to evaluate the reliability of the fitted power law function in describing the data (κ∈[0,∞], κ=0 denotes the highest reliability). The KS statistic κ indicates how likely the data are to be drawn from a power law. Figures 1a-1c show that the histograms of the number of case studies are significantly skewed toward lower values of κ for all cases of daily streamflows, ordinary peak flows, and monthly flow maxima with a > 2 (red histograms), whereas this is not true for cases with a < 2 (green histograms). Statistical significance of the skewnesses was evaluated through the Jarque–Bera test at a significance level of 0.05. The result essentially indicates that data from case studies which are identified with heavy-tailed behavior according to the hydrogeomorphological index (a>2, red) are indeed more likely to come from power law distributions.

We further estimate the accuracy of the hydrogeomorphological index based on the fraction of case studies that are correctly identified by the hydrogeomorphological index among all heavy-tailed cases. To define the number of cases with heavy tails based on the available observations, we choose a threshold value of κ to determine whether the data are reliably described by power law functions. Mathematically, the accuracy can be expressed as $P_{a>2}(\kappa < \kappa_r) = N_p(a > 2)/N_p$, where κ_r is the imposed threshold of κ, N_p is the number of case studies whose $\kappa < \kappa_r$, and $N_p(a > 2)$ is the number of case studies with $a > 2$ among the N_p case studies. Higher accuracy essentially means that a higher fraction of heavy-tailed cases (as defined by fitted power laws and a set κ_r threshold) are correctly identified by means of the hydrogeomorphological index. Notice that the smaller the κ_r threshold, the more reliable the description of power law distributions for data. The blue frame and dot in figures 1a and 1d display an example of defined reliability and the corresponding accuracy.

Figures 1d-1f display the accuracy of the hydrogeomorphological index as a function of the reliability threshold κ_r. In all three cases (daily streamflows, ordinary peak flows, and monthly flow maxima), the accuracy values increase with the reliability level of the power law function fitted on observed data. This means that the hydrogeomorphological index shows higher accuracy for case studies where the empirical distributions of observed data are more consistent with power laws. In other words, the proposed hydrogeomorphological index, which is estimated as the hydrograph recession exponent from commonly available daily flow records, is a robust indicator of heavy-tailed flood behavior.

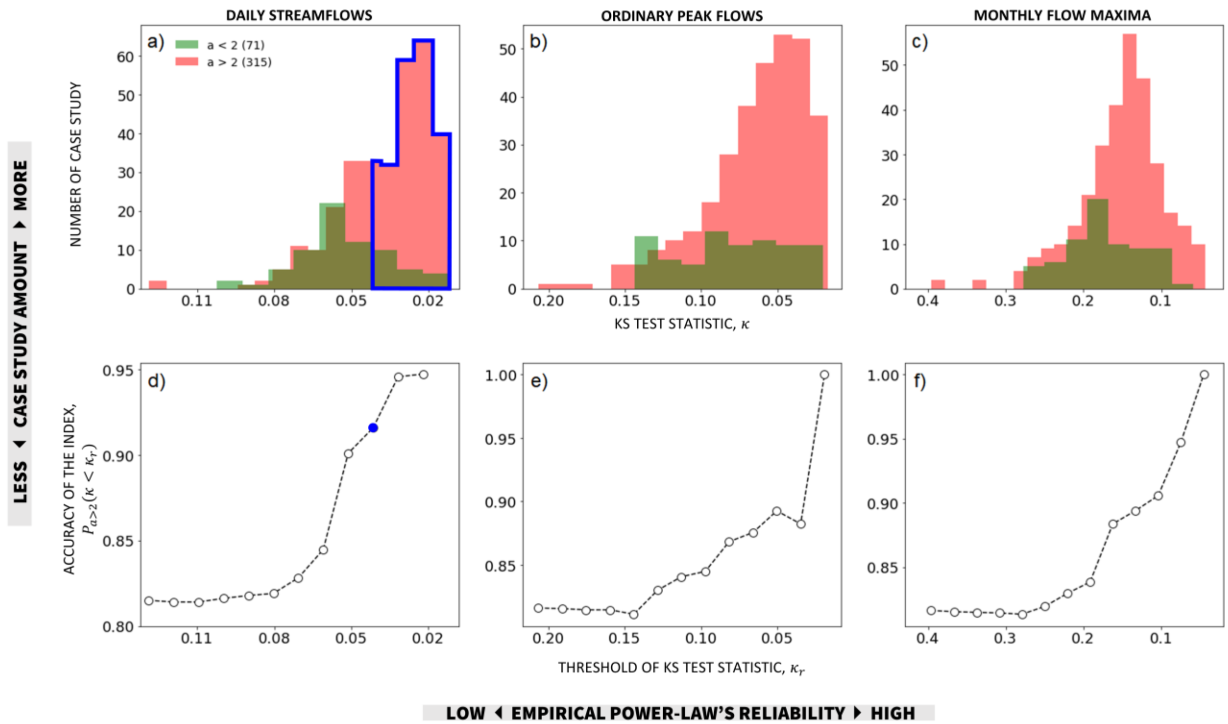

Figure 1. Accuracy of the proposed hydrogeomorphological index. (a)-(c) Number of analyzed case studies as a function of the KS statistic κ of empirically fitted power law distributions (the latter is a measure of how reliable the power law is as a model for the given data: the lower κ, the more reliable the power law model). Case studies are identified with either heavy- ($a > 2$, red histograms) or nonheavy ($a < 2$, green histograms) –tailed behavior based on the hydrograph recession exponent a estimated from daily flow records, which is proposed as a hydrogeomorphological index of heavy-tailed streamflow and flood behavior. (d)-(f) Accuracy of the hydrogeomorphological index as a function of decreasing thresholds of κ_r (i.e., increasing reliability of empirical power laws). The accuracy $P_{a>2}(\kappa < \kappa_r)$ is essentially the fraction of the red area under a specified threshold of κ (as explanatorily shown by the blue frames and dots in panels a and d). The values of the KS statistic κ are derived from records of (a, d) daily streamflows, (b, e) ordinary peak flows, and (c, f) monthly flow maxima.

We further employ the goodness-of-fit testing procedure proposed by Clauset et al. (2009) (supporting information Text S2) to identify case studies for which the representation of daily streamflow, ordinary peak flows, and monthly maxima by means of power law distributions is convincingly supported by the available data. We refer to these case studies as ‘confirmed heavy-tailed cases’ (Figure 2, black dots). Conversely, we term the remaining ones as 'uncertain cases' (Figure 2, gray). The latter label denotes that the distribution underlying the available observations may or may not be a power law but, statistically speaking, we cannot be conclusive due to data scarcity.

Figure 2 shows the empirical power law exponent b as a function of the hydrogeomorphological index of heavy-tailed flow behavior a. Red markers display the median values of a and b (squares), the interquartile intervals of b (vertical bars), and the binning ranges of a (horizontal bars, equal number of case studies in each bin), highlighting the correlation between the empirical power law exponent b and the hydrograph recession exponent a for confirmed heavy-tailed cases (black dots) in all three cases (i.e., daily streamflows, ordinary peak flows, and monthly flow maxima). We also test the correlation by calculating their distance correlation (Székely et al., 2007), which is valid for both potential linear and nonlinear associations between two random variables. We find that a and b are significantly correlated at a significance level of 0.05 in all three cases with distance (Spearman) correlation coefficients of 0.45, 0.44, and 0.81 (0.42, 0.46, and 0.60) for daily streamflows, ordinary peak flows, and monthly flow maxima. The last high value of correlation is likely affected by the existence of two clusters of black dots in Figure 2c. Nonetheless, the existence of a statistically significant correlation between the empirical power law exponent and the hydrogeomorphological index (confirmed for all panels a,b,c) confirms that the latter not only can be used to identify heavy-tailed flood behavior but also to evaluate the degree of the tail heaviness of the underlying distributions.

Figure 2c is of particular interest because it shows a common issue in the practice of flood hazard assessment. The power law is a plausible representation of the empirical distribution of monthly maxima in some cases (black dots) that are characterized by large values of the recession exponent a and are therefore classified as having heavy-tailed behavior according to the hydrogeomorphological index. In other cases (gray dots), conclusive evidence of possible heavy-tailed flood behavior cannot be drawn from the limited observations of monthly maxima. However, the hydrogeomorphological index retains its capability to provide estimates of the tail heaviness based on the value of the hydrograph recession exponent and classifies the case studies as heavy-tailed. Such a classification is deemed robust, provided that the predictions of the hydrogeomorhological index are confirmed by observations in cases (panels a and b) where data size is not a limitation (i.e., for daily streamflow and ordinary peak flows). The ability of the hydrogeomorphological index to infer the tail heaviness of flood distributions by examining the intrinsic dynamics of the hydrological system constitutes an advantage of the approach, that is especially useful in the very common cases when the tail of the flood distribution cannot be known from limited observations of maxima only.

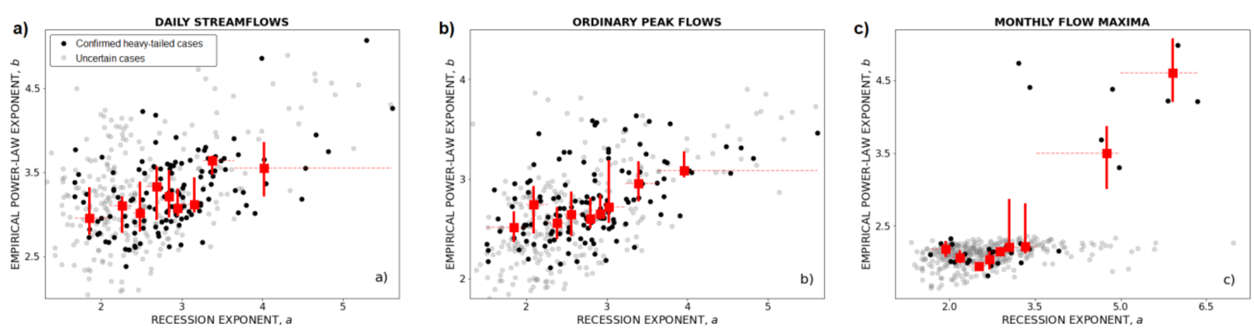

Figure 2. Empirical power law exponent b as a function of the hydrogeomorphological index of heavy-tailed behavior a. Case studies are classified into groups of confirmed heavy-tailed (black dots) and uncertain (gray dots) cases on the basis of the goodness-of-fit testing procedure (Clauset et al., 2009). The former denotes cases for which a power law provides a reliable description of the empirical data distribution, while the latter denotes cases whose data cannot convincingly support such a distribution. Red markers highlight the correlation between the empirical power law exponent b and the hydrograph recession exponent a for confirmed heavy-tailed cases in the case of (a) daily streamflows (n=121 case studies), (b) ordinary peak flows (n=116), and (c) monthly flow maxima (n=34). Red markers display the median values

of a and b (squares), the interquartile intervals of b (vertical bars), and the binning ranges of a (horizontal bars, equal number of case studies in each bin).

In Figure 3, we test the index stability of the categorization of case studies into heavy/nonheavy-tailed flood behavior for decreasing data lengths. We benchmark the hydrogeomorphological index (i.e., the hydrograph recession exponent a) against two other frequently used metrics of heavy tails in hydrological studies: (1) the upper tail ratio (UTR) (Lu et al., 2017; Smith et al., 2018; Villarini et al., 2011; Wang et al., 2022) and (2) the shape parameter ξ of the GEV distribution (Morrison & Smith, 2002; Papalexiou et al., 2013; Villarini & Smith, 2010). The UTR is derived as the ratio of the maximum record to the 0.9 quantiles of floods (Smith et al., 2018), and the ξ is estimated using the python package OpenTURNS 1.16 (Baudin et al., 2017). We compute both using data of monthly flow maxima. For all three indices ($a, UTR,$ and ξ), we estimate the index for decreasing data lengths from 35 (bounded by the shortest record length in the dataset) to 2 years in each case study. The index for each test length is calculated based on the median value of the estimates derived from 30 random fragments (with the assigned test length) of the entire record.

To have the reference of the stability of the categorization, we use the entire data record computing the values of the hydrogeomorphological index and the GEV shape parameter (notations with an asterisk in Figure 3, i.e., a^* and ξ^*). Each case study is categorized as either having (red) or not (green) the heavy-tailed behavior by the criteria of heavy (nonheavy) tails for the geomorphological index as $a^* > 2$ ($a^* < 2$) or for the GEV shape parameter as $\xi^* > 0$ ($\xi^* \leq 0$) (Godrèche et al., 2015). For the UTR, however, there is no specific threshold for the identification of heavy/nonheavy tails, but a larger value indicates a heavier tail.

The categorization of the hydrogeomorphological index is consistent across the test data length (Figure 3a). Specifically, the index estimates retain beyond 2 for most heavy-tailed cases (red) and below 2 for most nonheavy-tailed cases (green) when the data length decreases. The vertical shaded bar and line show the 0.25–0.75 and 0.05–0.95 quantile ranges of the index estimates across case studies. Besides the consistent categorization, the index estimates vary in a narrow range over the test data length both for the median value (i.e., from 2.64 to 2.92 for heavy-tailed cases and from 1.84 to 2.0 for nonheavy-tailed cases) and for the variation (e.g., the coefficient of variation ranges from 0.29 to 0.33 for heavy-tailed cases and from 0.29 to 0.33 for nonheavy-tailed cases). The small fluctuation of the variation across the test data length implies that the variation in index estimates is primarily caused by case study heterogeneity rather than decreasing data length. These results essentially confirm the stability of the hydrogeomorphological index for decreasing data lengths.

In contrast, the upper tail ratio shows pronounced instability for decreasing data lengths (Figure 3b). The median value of the index estimates ranges from 1.32 to 2.36, and the coefficient of variation ranges from 0.15 to 0.64, indicating that the tail heaviness is underestimated as data length decreases, in agreement with Smith et al. (2018) and Wietzke et al. (2020). The differential variation for decreasing data length denotes an apparent bias in the index estimates caused by the short data in addition to the heterogeneity across case studies.

Figure 3c shows the categorization of tail behavior based on the estimates of the GEV shape parameters. When the test data length is above five years, case studies with index estimates in the interquartile range (the vertical shaded bar) are consistent in the categorization of heavy/nonheavy-tailed behavior. When the data length is below five years, the underestimation of tail heaviness exists. Meanwhile, the index estimate changes slightly in its median but evidently in its coefficient of variation across the test data length. The former (latter) ranges from 0.39 to 0.52 (0.37 to 1.03) for the heavy-tailed cases and keeps 0 (--; the coefficient of variation is not applied for data with zero mean) for the nonheavy-tailed cases. These results show that the GEV shape parameter may still be considered a practical index for the heavy/nonheavy-tailed categorization because most applications have data that are more than five years. Nonetheless, the bias in the variation of index estimates across data length and the apparent underestimation in cases with very limited data point to the dependence on data lengths, in agreement with Papalexiou and Koutsoyiannis (2013).

We demonstrate the hydrogeomorphological index is robust in cases with limited data, i.e., it is stable in the categorization of heavy/nonheavy-tailed flood behavior for decreasing data lengths. Given that most data records worldwide are relatively short (Lins, 2008), this is a valuable tool to infer the tail behavior of streamflow in river basins. Moreover, given that generally all available records are too short of estimating the tail behavior of maxima (e.g., floods), this approach is even more valuable because it allows scientists or engineers to estimate the heavy-tailed flood behavior and assess the hazards from common discharge dynamics.

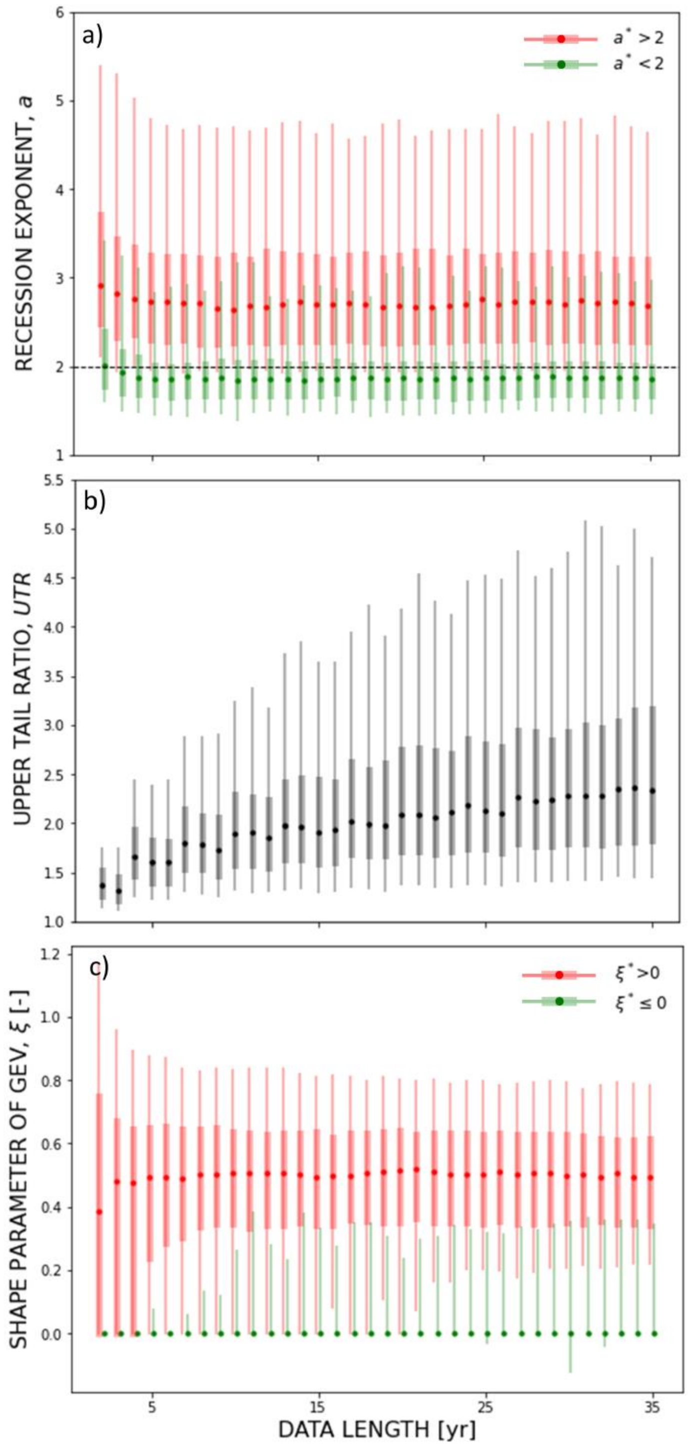

Figure 3. Stability of the categorization of case studies into heavy/nonheavy-tailed flood behavior for decreasing data lengths. Estimates of three different indices of tail behavior as a function of data length. (a) Hydrograph recession exponent a (i.e., the proposed hydrogeomorphological index of this study). Two frequently used metrics of heavy tails in hydrological studies: (b) the upper tail ratio UTR, and (c) the shape

parameter ξ of the GEV distribution. Dots display the median values of the estimates for 386 case studies; vertical shaded bars and lines respectively show the 0.25-0.75 and 0.05-0.95 quantile ranges of the estimates. The entire data record was used for computing the reference values of the hydrograph recession exponent a^* and the GEV shape parameter ξ^* and categorizing each case study as either having (red) or not (green) the heavy-tailed behavior.

5 Conclusions

The hydrograph recession exponent is identified as an index of heavy-tailed flood behavior from a physically-based description of hydrological dynamics. It is essentially a hydrogeomorphological index of heavy-tailed flood behavior because it originates from the geomorphological structure of the contributing river basin. We show that the proposed hydrogeomorphological index enables the identification of heavy/nonheavy-tailed flood behavior and the evaluation of the tail heaviness across case studies. Remarkably, it leverages the information of common discharge dynamics and shows robust identification of tail behavior for decreasing data length. We demonstrate all these capabilities in a large set of case studies across Germany on a seasonal basis, featuring the diversity in climatic and physiographic conditions. The hydrogeomorphological index addresses the limitations of other frequently used indices (e.g., lack of physical support, low effectiveness/ineffectiveness in cases with limited data) and allows for robust identification of heavy-tailed flood behavior, which is particularly useful in assessing hazards of extreme floods in data-scarce areas.

Acknowledgments

This work is funded by the Deutsche Forschungsgemeinschaft-Project 421396820 “Propensity of rivers to extreme floods: climate-landscape controls and early detection (PREDICTED)” and FOR 2416 “Space-Time Dynamics of Extreme Floods (SPATE)”. The financial support of the Helmholtz Centre for Environmental Research and the Norwegian Institute for Water Research is as well acknowledged. SY (the 3rd author) acknowledges the support of the Helmholtz Climate Initiative Project funded by the Helmholtz Association. The manuscript and supporting information provide all the information needed to replicate the results.

Data Availability Statement

For providing the discharge data for Germany, we are grateful to the Bavarian State Office of Environment (LfU, https://www.gkd.bayern.de/de/fluesse/abfluss) and the Global Runoff Data Centre (GRDC) prepared by the Federal Institute for Hydrology (BfG, http://www.bafg.de/GRDC). Climatic data can be obtained from the German Weather Service (DWD; ftp://ftp-cdc.dwd.de/pub/CDC/). The digital elevation model can be retrieved from Shuttle Radar Topography Mission (SRTM; https://cgiarcsi.community/data/srtm-90m-digital-elevation-database-v4-1/).

References

Arai, R., Toyoda, Y., & Kazama, S. (2020). Runoff recession features in an analytical probabilistic streamflow model. *Journal of Hydrology*, *597*, 125745. https://doi.org/10.1016/j.jhydrol.2020.125745

Basso, S., Botter, G., Merz, R., & Miniussi, A. (2021). PHEV! The PHysically-based Extreme Value distribution of river flows. *Environmental Research Letters*, *16*(12). https://doi.org/10.1088/1748-9326/ac3d59

Basso, S., Schirmer, M., & Botter, G. (2015). On the emergence of heavy-tailed streamflow distributions. *Advances in Water Resources*, *82*, 98–105. https://doi.org/10.1016/j.advwatres.2015.04.013

Basso, S., Schirmer, M., & Botter, G. (2016). A physically based analytical model of flood frequency curves. *Geophysical Research Letters*, *43*(17), 9070–9076. https://doi.org/10.1002/2016GL069915

Baudin, M., Dutfoy, A., Iooss, B., & Popelin, A.-L. (2017). OpenTURNS: An Industrial Software for Uncertainty Quantification in Simulation BT - Handbook of Uncertainty Quantification. In R. Ghanem, D. Higdon, & H. Owhadi (Eds.) (pp. 2001–2038). Cham: Springer International Publishing. https://doi.org/10.1007/978-3-319-12385-1_64

Beirlant, J., Goegebeur, Y., Teugels, J., Segers, J., De Waal, D., & Ferro, C. (2004). *Statistics of extremes: Theory and applications*. *Wiley*. https://doi.org/https://doi.org/10.1002/0470012382

Bernardara, P., Schertzer, D., Sauquet, E., Tchiguirinskaia, I., & Lang, M. (2008). The flood probability distribution tail: How heavy is it? *Stochastic Environmental Research and Risk Assessment*, *22*(1), 107–122. https://doi.org/10.1007/s00477-006-0101-2

Bevere, L., & Remondi, F. (2022). *Natural catastrophes in 2021: the floodgates are open*. *Swiss Re Institute sigma research*.

Biswal, B. (2021). Decorrelation is not dissociation: There is no means to entirely decouple the Brutsaert-Nieber parameters in streamflow recession analysis. *Advances in Water Resources*, *147*, 103822. https://doi.org/https://doi.org/10.1016/j.advwatres.2020.103822

Biswal, B., & Marani, M. (2010). Geomorphological origin of recession curves. *Geophysical Research Letters*, *37*(24), 1–5. https://doi.org/10.1029/2010GL045415

Biswal, B., & Marani, M. (2014). “Universal” recession curves and their geomorphological interpretation. *Advances in Water Resources*, *65*, 34–42. https://doi.org/10.1016/j.advwatres.2014.01.004

Biswal, B., & Nagesh Kumar, D. (2014). What mainly controls recession flows in river basins? *Advances in Water Resources*, *65*, 25–33. https://doi.org/10.1016/j.advwatres.2014.01.001

Botter, G., Basso, S., Porporato, A., Rodriguez-Iturbe, I., & Rinaldo, A. (2010). Natural streamflow regime alterations: Damming of the Piave river basin (Italy). *Water Resources Research*, *46*(6), 1–14. https://doi.org/10.1029/2009WR008523

Botter, G., Peratoner, F., Porporato, A., Rodriguez-Iturbe, I., & Rinaldo, A. (2007). Signatures of large-scale soil moisture dynamics on streamflow statistics across U.S. climate regimes. *Water Resources Research*, *43*(11), 1–10. https://doi.org/10.1029/2007WR006162

Botter, G., Porporato, A., Rodriguez-Iturbe, I., & Rinaldo, A. (2007). Basin-scale soil moisture dynamics and the probabilistic characterization of carrier hydrologic flows: Slow, leaching-prone components of the hydrologic response. *Water Resources Research*, *43*(2), 1–14. https://doi.org/10.1029/2006WR005043

Botter, G., Porporato, A., Rodriguez-Iturbe, I., & Rinaldo, A. (2009). Nonlinear storage-discharge relations and catchment streamflow regimes. *Water Resources Research*, *45*(10), 1–16. https://doi.org/10.1029/2008WR007658

Brutsaert, W., & Nieber, J. L. (1977). Regionalized drought flow hydrographs from a mature glaciated plateau. *Water Resources Research*, *13*(3), 637–643. https://doi.org/10.1029/WR013i003p00637

Ceola, S., Botter, G., Bertuzzo, E., Porporato, A., Rodriguez-Iturbe, I., & Rinaldo, A. (2010). Comparative study of ecohydrological streamflow probability distributions. *Water Resources Research*, *46*(9), 1–12. https://doi.org/10.1029/2010WR009102

Clauset, A., Shalizi, C. R., & Newman, M. E. J. (2009). Power-law distributions in empirical data. *SIAM Review*, *51*(4), 661–703. https://doi.org/10.1137/070710111

Cooke, R. M., Nieboer, D., & Misiewicz, J. (2014). *Fat-Tailed Distributions: Data, Diagnostics and Dependence* (volume 1). John Wiley & Sons.

Cooke, R. M., & Nieboer, D. (2011). Heavy-Tailed Distributions: Data, Diagnostics, and New Developments. *Resources for the Future Discussion Paper, No. 11-19*. https://doi.org/dx.doi.org/10.2139/ssrn.1811043

Doulatyari, B., Betterle, A., Basso, S., Biswal, B., Schirmer, M., & Botter, G. (2015). Predicting streamflow distributions and flow duration curves from landscape and climate. *Advances in Water Resources*, *83*, 285–298. https://doi.org/10.1016/j.advwatres.2015.06.013

Durrans, S. R., Eiffe, M. A., Thomas, W. O., & Goranflo, H. M. (2003). Joint Seasonal /Annual Flood Frequency Analysis. *Journal of Hydrologic Engineering*, *8*(4), 181–189. https://doi.org/10.1061/(asce)1084-0699(2003)8:4(181)

El Adlouni, S., Bobée, B., & Ouarda, T. B. M. J. (2008). On the tails of extreme event distributions in hydrology. *Journal of Hydrology*, *355*(1–4), 16–33. https://doi.org/10.1016/j.jhydrol.2008.02.011

Eliazar, I., & Sokolov, I. (2010). Gini characterization of extreme-value statistics. *Physica A-Statistical Mechanics and Its Applications - PHYSICA A*, *389*, 4462–4472. https://doi.org/10.1016/j.physa.2010.07.005

Else, H. (2021). Climate change implicated in Germany's deadly floods. *Nature*. https://doi.org/10.1038/d41586-021-02330-y

Embrechts, P., Klüppelberg, C., & Mikosch, T. (1997). *Modelling extreme events for insurance and finance*. Springer Berlin Heidelberg.

Fischer, S., & Schumann, A. (2016). Robust flood statistics: comparison of peak over threshold approaches based on monthly maxima and TL-moments. *Hydrological Sciences Journal*, *61*(3), 457–470. https://doi.org/10.1080/02626667.2015.1054391

Ghosh, D. K., Wang, D., & Zhu, T. (2016). On the transition of base flow recession from early stage to late stage. *Advances in Water Resources*, *88*, 8–13. https://doi.org/10.1016/j.advwatres.2015.11.015

Godrèche, C., Majumdar, S. N., & Schehr, G. (2015). Statistics of the longest interval in renewal processes. *Journal of Statistical Mechanics: Theory and Experiment*, *2015*(3). https://doi.org/10.1088/1742-5468/2015/03/P03014

Jachens, E. R., Rupp, D. E., Roques, C., & Selker, J. S. (2020). Recession analysis revisited: Impacts of climate on parameter estimation. *Hydrology and Earth System Sciences*, *24*(3), 1159–1170. https://doi.org/10.5194/hess-24-1159-2020

Katz, R. (2002). Statistics of Extremes in Climatology and Hydrology. *Advances in Water Resources*, *25*, 1287–1304.

Kondor, D., Pósfai, M., Csabai, I., & Vattay, G. (2014). Do the rich get richer? An empirical analysis of the Bitcoin transaction network. *PLoS ONE*, *9*(2). https://doi.org/10.1371/journal.pone.0086197

Laio, F., Porporato, A., Fernandez-Illescas, C. P., & Rodriguez-Iturbe, I. (2001). Plants in water-controlled ecosystems: Active role in hydrologic processes and responce to water stress IV. Discussion of real cases. *Advances in Water Resources*, *24*(7), 745–762. https://doi.org/10.1016/S0309-1708(01)00007-0

Lins, H. F. (2008). Challenges to hydrological observations. *WMO Bulletin*, *57*(January), 55–58.

Lu, P., Smith, J. A., & Lin, N. (2017). Spatial characterization of flood magnitudes over the drainage network of the Delaware river basin. *Journal of Hydrometeorology*, *18*(4), 957–976. https://doi.org/10.1175/JHM-D-16-0071.1

Malamud, B. D. (2004). Tails of natural hazards. *Physics World*, *17*(8), 31–35. https://doi.org/10.1088/2058-7058/17/8/35

Malamud, B. D., & Turcotte, D. L. (2006). The applicability of power-law frequency statistics to floods. *Journal of Hydrology*, *322*(1–4), 168–180. https://doi.org/10.1016/j.jhydrol.2005.02.032

McDermott, T. K. J. (2022). Global exposure to flood risk and poverty. *Nature Communications*, *13*(1), 6–8. https://doi.org/10.1038/s41467-022-30725-6

Mejía, A., Daly, E., Rossel, F., Javanovic, T., & Gironás, J. (2014). A stochastic model of streamflow for urbanized basins. *Water Resources Research*, *50,* 1984–2001. https://doi.org/10.1002/2013WR014834

Merz, B., Basso, S., Fischer, S., Lun, D., Blöschl, G., Merz, R., et al. (2022). Understanding heavy tails of flood peak distributions. *Water Resources Research*, 1–37. https://doi.org/10.1029/2021wr030506

Merz, B., Blöschl, G., Vorogushyn, S., Dottori, F., Aerts, J. C. J. H., Bates, P., et al. (2021). Causes, impacts and patterns of disastrous river floods. *Nature Reviews Earth and Environment*, *2*(9), 592–609. https://doi.org/10.1038/s43017-021-00195-3

Merz, R., & Blöschl, G. (2009). Process controls on the statistical flood moments - a data based analysis. *Hydrological Processes*, *23*(5), 675–696. https://doi.org/10.1002/hyp

Morrison, J. E., & Smith, J. A. (2002). Stochastic modeling of flood peaks using the generalized extreme value distribution. *Water Resources Research, 38*(12), 41-1-41–12. https://doi.org/10.1029/2001wr000502

Müller, M. F., Dralle, D. N., & Thompson, S. E. (2014). Analytical model for flow duration curves in seasonally dry climates. *Water Resources Research*, *50*, 5510–5531. https://doi.org/10.1002/2014WR015301

Müller, M. F., Roche, K. R., & Dralle, D. N. (2021). Catchment processes can amplify the effect of increasing rainfall variability. *Environmental Research Letters*, *16*(8). https://doi.org/10.1088/1748-9326/ac153e

Mutzner, R., Bertuzzo, E., Tarolli, P., Weijs, S. V., Nicotina, L., Ceola, S., et al. (2013). Geomorphic signatures on Brutsaert base flow recession analysis. *Water Resources Research*, *49*(9), 5462–5472. https://doi.org/10.1002/wrcr.20417

Nerantzaki, S. D., & Papalexiou, S. M. (2019). Tails of extremes: Advancing a graphical method and harnessing big data to assess precipitation extremes. *Advances in Water Resources*, *134*. https://doi.org/10.1016/j.advwatres.2019.103448

Papalexiou, S. M., Koutsoyiannis, D., & Makropoulos, C. (2013). How extreme is extreme? An assessment of daily rainfall distribution tails. *Hydrology and Earth System Sciences*, *17*(2), 851–862. https://doi.org/10.5194/hess-17-851-2013

Papalexiou, S. M., & Koutsoyiannis, D. (2013). Battle of extreme value distributions : A global survey on extreme daily rainfall. *Water Resources Research*, *49*(1), 187–201. https://doi.org/10.1029/2012WR012557

Porporato, A., Daly, E., & Rodriguez-Iturbe, I. (2004). Soil water balance and ecosystem response to climate change. *American Naturalist*, *164*(5), 625–632. https://doi.org/10.1086/424970

Pumo, D., Viola, F., La Loggia, G., & Noto, L. V. (2014). Annual flow duration curves assessment in ephemeral small basins. *Journal of Hydrology*, *519*(PA), 258–270. https://doi.org/10.1016/j.jhydrol.2014.07.024

Rajah, K., O'Leary, T., Turner, A., Petrakis, G., Leonard, M., & Westra, S. (2014). Changes to the temporal distribution of daily precipitation. *Geophysical Research Letters*, *41*(24), 8887–8894. https://doi.org/10.1002/2014GL062156

Rentschler, J., Salhab, M., & Jafino, B. A. (2022). Flood exposure and poverty in 188 countries. *Nature Communications*, *13*(1), 3527. https://doi.org/10.1038/s41467-022-30727-4

Resnick, S. I. (2007). *Heavy-Tail Phenomena: Probabilistic and Statistical Modeling*. New York: Springer US.

Santos, A. C., Portela, M. M., Rinaldo, A., & Schaefli, B. (2018). Analytical flow duration curves for summer streamflow in Switzerland. *Hydrology and Earth System Sciences*, *22*(4), 2377–2389. https://doi.org/10.5194/hess-22-2377-2018

Sartori, M., & Schiavo, S. (2015). Connected we stand: A network perspective on trade and global food security. *Food Policy*, *57*, 114–127. https://doi.org/https://doi.org/10.1016/j.foodpol.2015.10.004

Schaefli, B., Rinaldo, A., & Botter, G. (2013). Analytic probability distributions for snow-dominated streamflow. *Water Resources Research*, *49*(5), 2701–2713. https://doi.org/10.1002/wrcr.20234

Smith, J. A., Cox, A. A., Baeck, M. L., Yang, L., & Bates, P. (2018). Strange Floods: The Upper Tail of Flood Peaks in the United States. *Water Resources Research*, *54*(9), 6510–6542. https://doi.org/10.1029/2018WR022539

Székely, G. J., Rizzo, M. L., & Bakirov, N. K. (2007). Measuring and testing dependence by correlation of distances. *Annals of Statistics*, *35*(6), 2769–2794. https://doi.org/10.1214/009053607000000505

Tarasova, L., Basso, S., & Merz, R. (2020). Transformation of Generation Processes From Small Runoff Events to Large Floods. *Geophysical Research Letters*, *47*(22). https://doi.org/10.1029/2020GL090547

Tashie, A., Pavelsky, T., & Band, L. E. (2020). An Empirical Reevaluation of Streamflow Recession Analysis at the Continental Scale. *Water Resources Research*, *56*(1), 1–18. https://doi.org/10.1029/2019WR025448

Tashie, A., Pavelsky, T., & Emanuel, R. E. (2020). Spatial and Temporal Patterns in Baseflow Recession in the Continental United States. *Water Resources Research*, *56*(3), 1–18. https://doi.org/10.1029/2019WR026425

Tashie, A., Scaife, C. I., & Band, L. E. (2019). Transpiration and subsurface controls of streamflow recession characteristics. *Hydrological Processes*, *33*(19), 2561–2575. https://doi.org/10.1002/hyp.13530

Vázquez, A., Oliveira, J. G., Dezsö, Z., Goh, K. Il, Kondor, I., & Barabási, A. L. (2006). Modeling bursts and heavy tails in human dynamics. *Physical Review E - Statistical, Nonlinear, and Soft Matter Physics*, *73*(3), 1–19. https://doi.org/10.1103/PhysRevE.73.036127

Villarini, G., & Smith, J. A. (2010). Flood peak distributions for the eastern United States. *Water Resources Research*, *46*(6), 1–17. https://doi.org/10.1029/2009WR008395

Villarini, G., Smith, J. A., Baeck, M. L., Marchok, T., & Vecchi, G. A. (2011). Characterization of rainfall distribution and flooding associated with U.S. landfalling tropical cyclones: Analyses of Hurricanes Frances, Ivan, and Jeanne (2004). *Journal of Geophysical Research Atmospheres*, *116*(23). https://doi.org/10.1029/2011JD016175

Wang, H., Merz, R., Yang, S., Tarasova, L., & Basso, S. (2022). Emergence of heavy tails in streamflow distributions: the role of spatial rainfall variability. *Advances in Water Resources Journal*, *171*(104359). https://doi.org/10.1016/j.advwatres.2022.104359

Wietzke, L. M., Merz, B., Gerlitz, L., Kreibich, H., Guse, B., Castellarin, A., & Vorogushyn, S. (2020). Comparative analysis of scalar upper tail indicators. *Hydrological Sciences Journal*, *65*(10), 1625–1639. https://doi.org/10.1080/02626667.2020.1769104

Zorzetto, E., Botter, G., & Marani, M. (2016). On the emergence of rainfall extremes from ordinary events. *Geophysical Research Letters*, *43*(15), 8076–8082. https://doi.org/10.1002/2016GL069445

A hydrogeomorphological index of heavy-tailed flood behavior

H. -J. Wang[1], R. Merz[1,2], S. Yang[3], and S. Basso[1,4]

[1]Department of Catchment Hydrology, Helmholtz Centre for Environmental Research – UFZ, Halle (Saale), Germany,

[2]Institute of Geosciences and Geography, Martin-Luther University Halle-Wittenberg, Halle (Saale), Germany,

[3]Department of Aquatic Ecosystem Analysis, Helmholtz Centre for Environmental Research – UFZ, Magdeburg, Germany

[4]Norwegian Institute for Water Research (NIVA), Oslo, Norway

Corresponding author: Hsing-Jui Wang (hsing-jui.wang@ufz.de)

Key Points:

- The hydrograph recession exponent is identified as an index of heavy-tailed flood behavior.
- The proposed index enables robust identification of heavy-tailed flood behavior in a large set of case studies and from short data records.
- Unlike other frequently used metrics, the proposed index infers heavy-tailed flood behaviors from commonly observed discharge dynamics.

Abstract

Floods are often disastrous due to underestimation of the magnitude of rare events. When the occurrence of floods follows a heavy-tailed distribution the chance of extreme events is sizable. However, identifying heavy-tailed flood behavior is challenging because of limited data records and the lack of physical support for currently used indices. We address these issues by deriving a new index of heavy-tailed flood behavior from a physically-based description of streamflow dynamics. The proposed index, which is embodied by the hydrograph recession exponent, enables inferring heavy-tailed flood behavior from daily flow records. We test the index in a large set of case studies across Germany. Results show its ability to identify cases with either heavy- or nonheavy-tailed flood behavior, and to evaluate the tail heaviness. Remarkably, the results are robust also for decreasing the lengths of data records. The new index thus allows for assessing flood hazards from commonly available data.

Plain Language Summary

High flow events often cause severe damages when they occur unexpectedly, i.e., more often and with larger magnitudes than suggested by historical observations. This is usually the case with frequency distributions of floods which are heavy-tailed. However, a proper assessment of the tail behavior solely based on limited data records is difficult and might lead to an erroneous estimation of the underlying hazard. We start by analyzing runoff generation processes and find that the hydrograph recession is a proper descriptor of the emergence of heavy-tailed behavior. Our findings show that the new proposed index allows for (1) detecting cases with heavy-tailed behavior, (2) comparing severity across cases, and (3) displaying robust results also with short data records. These results address the main limitations of currently used metrics (which often require long records and lack physical meaning) and provide information on the characteristic flood hazard of river basins.

1 Introduction

Floods remain the leading natural hazards worldwide, which directly threaten at least one-fifth of people's livelihoods (McDermott, 2022; Rentschler et al., 2022) and have caused enormous and increasing economic losses (Bevere & Remondi, 2022) in recent years. Floods are often disastrous because they occur unexpectedly (i.e., underestimated by water resources managers as well as residents) (Else, 2021; Merz et al., 2021), commonly due to poor estimates of the magnitude of rare events obtained from available observations. A number of studies in natural and anthropogenic phenomena use heavy-tailed distributions to describe the extreme behavior of variables (e.g., Katz, 2002; Kondor et al., 2014; Malamud, 2004; Sartori & Schiavo, 2015; Wang et al., 2022) because it indicates a sizable chance of the occurrence of extreme value. We can better assess the flood hazards if we may know that floods follow a heavy-tailed distribution, i.e., robustly identify the heavy-tailed flood behavior (Merz et al., 2022).

A variable distribution's tail heaviness is traditionally estimated graphically or mathematically, while both have their limitations. In general, graphical methods such as log-log plots (Beirlant et al., 2004), generalized Hill ratio plots (Resnick, 2007; El Adlouni et al., 2008), and mean excess functions (Embrechts et al., 1997; Nerantzaki & Papalexiou, 2019) have less objectivity and efficiency (Cooke et al., 2014). Mathematical methods provide more objective insights into the estimation of tail behavior. The shape parameters of Generalized Extreme Value (GEV) distributions quantify the tail behavior by fitting the parameters of an underlying distribution on limited records of maxima (Morrison & Smith, 2002; Villarini & Smith, 2010; Papalexiou et al., 2013), and a group of non-parametric metrics evaluates the spread of data (e.g., upper tail ratio (Lu et al., 2017; Smith et al., 2018; Villarini et al., 2011; Wang et al., 2022), Gini index (Eliazar & Sokolov, 2010; Rajah et al., 2014), and obesity index (Cooke & Nieboer, 2011; Sartori & Schiavo, 2015)). These methods often require long records to obtain reliable estimates (Papalexiou & Koutsoyiannis, 2013). This is a challenge globally and even more challenging when it comes to analyzing maxima (which is indeed the key to assessing hazards of extreme floods). The bias caused by the data size restricts the comparability across sites with different record lengths (Wietzke et al., 2020). In addition, the correctness of the estimation of tail heaviness is influenced by the underlying physical processes of the case studies (Merz et al., 2022). However, to the best of our knowledge, physical processes are absent from these frequently used metrics. It is preferable to have a new index that can robustly estimate with data in different lengths (Bernardara et al., 2008; Merz & Blöschl, 2009) and is based on the physical processes that favor the heavy-tailed behavior of flood distributions.

We propose a new index of heavy-tailed flood behavior, which can be estimated by common discharge dynamics. Unlike fitting a statistical distribution to observed series of maxima (which may not clearly exhibit heavy-tailed behavior due to data scarcity), the index infers the tail heaviness of floods by examining the intrinsic dynamics of the hydrological system. Reliable identification of heavy tails by the proposed index is tested in datasets with decreasing lengths in a great number of case studies with various climate and physiographic features. We leverage common discharge dynamics to facilitate flood peril assessment and demonstrate its usefulness in areas with limited records.

2 Identifying tail behavior from hydrological dynamics

We describe key hydrologic dynamics occurring at the catchment scale and the resulting probability distributions of streamflow and floods by means of the PHysically-based Extreme Value (PHEV) distribution of river flows (Basso et al., 2021). This framework is grounded on a well-established mathematical description of precipitation, soil moisture, and runoff generation in river basins (Laio et al., 2001; Porporato et al., 2004; Botter et al., 2007b, 2009). Rainfall is described as a marked Poisson process with frequency $\lambda_p[\mathrm{T}^{-1}]$ and exponentially distributed depths with average α [L]. Soil moisture increases due to rainfall infiltration and decreases due to evapotranspiration. The latter is represented by a linear function of soil moisture between the wilting point and an upper critical value expressing the water holding capacity of the root zone. Runoff pulses occur with frequency $\lambda < \lambda_p$ when the soil moisture exceeds the critical value. These pulses replenish single catchment storage, which drains according to a nonlinear storage-discharge relation. The related hydrograph recession is described via a power law function with exponent a $[-]$ and coefficient K $[\mathrm{L}^{1-\mathrm{a}}/\mathrm{T}^{2-\mathrm{a}}]$ (Brutsaert & Nieber, 1977), which allows for mimicking the joint effect of different flow components (Basso et al., 2015). Such a description of runoff generation and streamflow dynamics was successfully tested in a variety of hydro-climatic and physiographic conditions (Arai et al., 2020; Botter et al., 2007a; Botter et al., 2010; Ceola et al., 2010; Doulatyari et al., 2015; Mejía et al., 2014; Müller et al., 2014; Müller et al., 2021; Pumo et al., 2014; Santos et al., 2018; Schaefli et al., 2013).

PHEV provides a set of consistent expressions for the probability distributions of daily streamflow, ordinary peak flows (i.e., local flow peaks occurring as a result of streamflow-producing rainfall events; Zorzetto et al., 2016), and floods (i.e., flow maxima in a certain timeframe; Basso et al., 2021). For example, the probability distribution of daily streamflow q can be expressed as (Botter et al., 2009):

$$p(q) = C_1 \cdot q^{-a}\left(e^{\frac{-1}{\alpha K(2-a)}\cdot q^{2-a}}\right)\left(e^{\frac{\lambda}{K(1-a)}\cdot q^{1-a}}\right) \tag{1}$$

where C_1 is a normalization constant.

Taking the limit of Equation (1) for $q \to +\infty$ gives indications of the tail behavior of the flow distribution (Basso et al., 2015). This is determined by the three terms in the equation, namely, one power law and two exponential functions, which behave differently depending on the value of the hydrograph recession exponent a (Equation 2; notice that $a > 1$ in most natural river basins; Tashie et al., 2020a).

$$\lim_{q\to+\infty} p(q) = \lim_{q\to+\infty}\left\{C_1 \cdot \overbrace{\underbrace{q^{-a}}_{\mapsto 0}}^{\mapsto 0}\overbrace{\underbrace{\left(e^{\frac{-1}{\alpha K(2-a)}\cdot q^{2-a}}\right)}_{\mapsto e^0 = 1}}^{\mapsto 0}\overbrace{\underbrace{\left(e^{\frac{\lambda}{K(1-a)}\cdot q^{1-a}}\right)}_{\mapsto e^0 = 1 \qquad \text{for } a > 2}}^{\mapsto e^0 = 1 \qquad \text{for } 1 < a < 2}\right\} \tag{2}$$

When $1 < a < 2$, the last term on the right-hand side converges to a constant value of one as q increases, thereby no more influence on how the distribution decreases toward zero. The first two terms instead decrease toward zero, affecting how the probability decreases for increasing values of q. The tail behavior is in this case determined by both a power law and an exponential functions, indicating that the probability decreases faster than an exponential but slower than a power law. When $a > 2$, both the exponential terms converge to a constant value of one as q increases, and thus no more influence on how the probability decreases toward zero. In this case the tail of the distribution is solely determined by the power law function. Despite being aware that several definitions of heavy-tailed distribution exist (El Adlouni et al., 2008; Vázquez et al., 2006), in the remaining of the manuscript we refer to heavy-tailed behavior for the case of distributions which exhibit a power law tail (i.e., the cases with a > 2). We thus aim to distinguish them from cases which display a lighter tail because of the simultaneous effect of exponential decay (i.e., the cases with $1 < a < 2$).

From the above derivations, the hydrograph recession exponent emerges as a key index of the tail behavior of streamflow distributions, which shall be heavy-tailed for values of $a > 2$. The same analysis applies to infer the tail behavior of the probability distributions of ordinary peak flows (Botter et al., 2009) and floods (Basso et al., 2016) (see supporting information Text S1). Remarkably, we find that the same critical value of the recession exponent indicates the emergence of heavy-tailed behavior also in peak flow and flood distributions. We therefore propose the hydrograph recession exponent a as an index for identifying heavy-tailed flood behavior, and test its capability to correctly predict such behavior in Section 4.

Recent studies showed that the hydrograph recession exponent is a convincing descriptor of the geomorphological signature of drainage areas (Biswal & Marani, 2010, 2014; Biswal & Kumar, 2014; Ghosh et al., 2016; Mutzner et al., 2013). The river network structure primarily defines how the geometry of saturated (Mutzner et al., 2013) and unsaturated areas (Biswal & Marani, 2010) of a river basin change over the draining process, which essentially determines the streamflow dynamics at the outlet. Despite being aware of the influences of seasonal climate (Jachens et al., 2020; Tashie et al., 2019), the geomorphological structure of the contributing river network has been demonstrated as the major determinator of the hydrograph recession exponent (Biswal & Kumar, 2014; Ghosh et al., 2016). We thus refer to the hydrograph recession exponent for a hydrogeomorphological index of heavy-tailed flood behavior.

3 Data and parameter estimation

To test the proposed hydrogeomorphological index of heavy-tailed flood behavior (i.e., the hydrograph recession exponent a), we use streamflow records with daily time resolution of 98 gauges across Germany (Figure S1). The analyzed river basins encompass a variety of climate and physiographic settings (Tarasova et al., 2020), while not being heavily affected by anthropogenic flow regulation and snow dynamics across seasons. Their areas range from 110 to 23,843 km^2 with a median value of 1,195 km^2. The minimum, median, and maximum lengths of the streamflow records are 35, 58, and 63 years (inbetween 1951 – 2013). We perform all analyses on a seasonal basis (winter: December–February, spring: March–May, summer: June–August, fall: September–November) to account for the seasonality of the hydrograph recessions and flood distributions (Durrans et al., 2003; Tashie et al., 2020b). This results in an overall number of 386 case studies used in our study.

We estimated a as the median value of the exponents of power law functions fitted to $dq/dt - q$ pairs of each hydrograph recession observed in the daily flow series (Jachens et al., 2020; Biswal, 2021). Notice that the proposed indicator of heavy-tailed flood behavior is thus estimated based on commonly available daily discharge observations.

The identification of case studies with either heavy- or nonheavy-tailed behavior resulting from the proposed index must be evaluated against a suitable benchmark. This is obtained by means of a state-of-the-art approach to fit power law functions to empirical distributions and evaluate their plausibility for the analyzed data (Clauset et al., 2009). The fitted exponent is here noted as b. We analyze three types of empirical data, namely daily streamflow, ordinary peaks, and monthly maxima (Fischer & Schumann, 2016; Malamud & Turcotte, 2006), and obtain estimates of the fitted exponent b for each case. These results will be used to validate the capabilities of the proposed hydrogeomorphological index to infer heavy-tailed flood behavior from the analysis of hydrograph recessions.

4 Results and discussion

We examine if power law distributions fitted to the empirical distributions of daily streamflow, ordinary peaks, and monthly maxima well describe the observed data for the case studies identified as having heavy-tailed behavior (i.e., a > 2) according to the hydrogeomorphological index (Figure 1). First, we identify the case studies with either heavy- (a > 2; red) or nonheavy (a < 2; green) -tailed behavior based on the hydrogeomorphological index. Then, we use the Kolmogorov-Smirnov (KS) statistic κ to evaluate the reliability of the fitted power law function in describing the data ($\kappa \in [0,\infty]$, $\kappa=0$ denotes the highest reliability). The KS statistic κ indicates how likely the data are to be drawn from a power law. Figures 1a-1c show that the histograms of the number of case studies are significantly skewed toward lower values of κ for all cases of daily streamflows, ordinary peak flows, and monthly flow maxima with a > 2 (red histograms), whereas this is not true for cases with a < 2 (green histograms). Statistical significance of the skewnesses was evaluated through the Jarque–Bera test at a significance level of 0.05. The result essentially indicates that data from case studies which are identified with heavy-tailed behavior according to the hydrogeomorphological index (a>2, red) are indeed more likely to come from power law distributions.

We further estimate the accuracy of the hydrogeomorphological index based on the fraction of case studies that are correctly identified by the hydrogeomorphological index among all heavy-tailed cases. To define the number of cases with heavy tails based on the available observations, we choose a threshold value of κ to determine whether the data are reliably described by power law functions. Mathematically, the accuracy can be expressed as $P_{a>2}(\kappa < \kappa_r) = N_p(a > 2)/N_p$, where κ_r is the imposed threshold of κ, N_p is the number of case studies whose $\kappa < \kappa_r$, and $N_p(a > 2)$ is the number of case studies with $a > 2$ among the N_p case studies. Higher accuracy essentially means that a higher fraction of heavy-tailed cases (as defined by fitted power laws and a set κ_r threshold) are correctly identified by means of the hydrogeomorphological index. Notice that the smaller the κ_r threshold, the more reliable the description of power law distributions for data. The blue frame and dot in figures 1a and 1d display an example of defined reliability and the corresponding accuracy.

Figures 1d-1f display the accuracy of the hydrogeomorphological index as a function of the reliability threshold κ_r. In all three cases (daily streamflows, ordinary peak flows, and monthly flow maxima), the accuracy values increase with the reliability level of the power law function fitted on observed data. This means that the hydrogeomorphological index shows higher accuracy for case studies where the empirical distributions of observed data are more consistent with power laws. In other words, the proposed hydrogeomorphological index, which is estimated as the hydrograph recession exponent from commonly available daily flow records, is a robust indicator of heavy-tailed flood behavior.

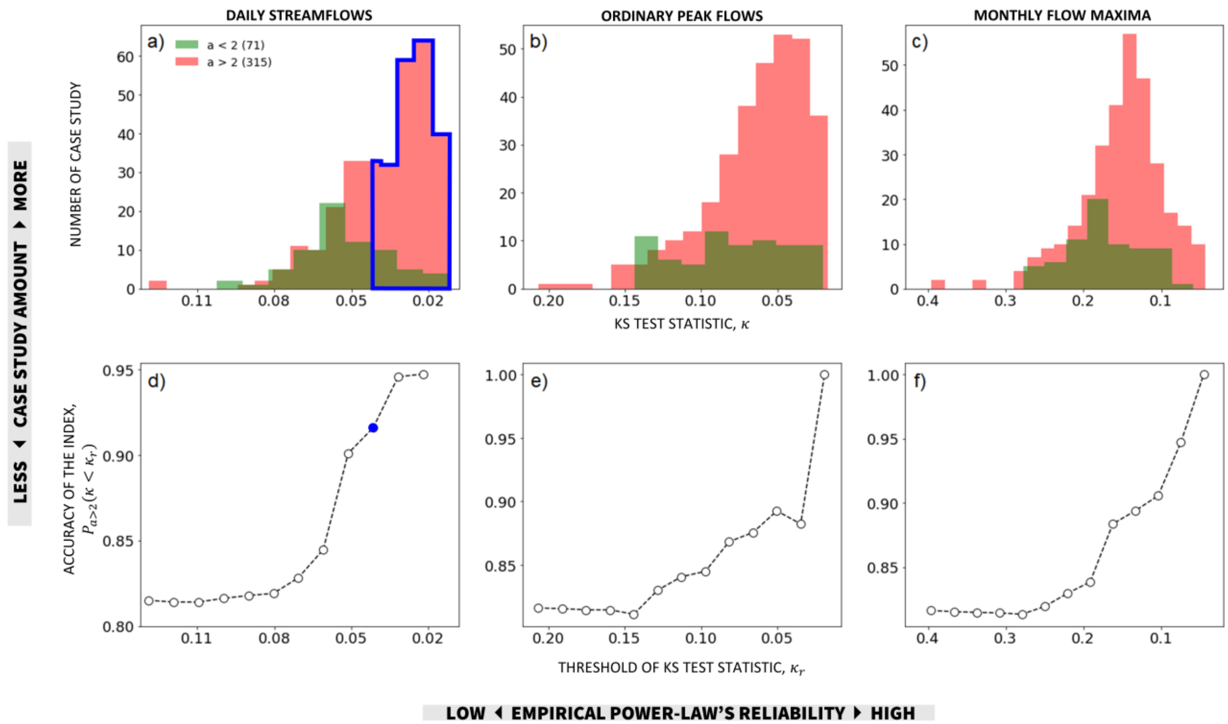

Figure 1. Accuracy of the proposed hydrogeomorphological index. (a)-(c) Number of analyzed case studies as a function of the KS statistic κ of empirically fitted power law distributions (the latter is a measure of how reliable the power law is as a model for the given data: the lower κ, the more reliable the power law model). Case studies are identified with either heavy- ($a > 2$, red histograms) or nonheavy ($a < 2$, green histograms) –tailed behavior based on the hydrograph recession exponent a estimated from daily flow records, which is proposed as a hydrogeomorphological index of heavy-tailed streamflow and flood behavior. (d)-(f) Accuracy of the hydrogeomorphological index as a function of decreasing thresholds of κ_r (i.e., increasing reliability of empirical power laws). The accuracy $P_{a>2}(\kappa < \kappa_r)$ is essentially the fraction of the red area under a specified threshold of κ (as explanatorily shown by the blue frames and dots in panels a and d). The values of the KS statistic κ are derived from records of (a, d) daily streamflows, (b, e) ordinary peak flows, and (c, f) monthly flow maxima.

We further employ the goodness-of-fit testing procedure proposed by Clauset et al. (2009) (supporting information Text S2) to identify case studies for which the representation of daily streamflow, ordinary peak flows, and monthly maxima by means of power law distributions is convincingly supported by the available data. We refer to these case studies as ‘confirmed heavy-tailed cases’ (Figure 2, black dots). Conversely, we term the remaining ones as 'uncertain cases' (Figure 2, gray). The latter label denotes that the distribution underlying the available observations may or may not be a power law but, statistically speaking, we cannot be conclusive due to data scarcity.

Figure 2 shows the empirical power law exponent b as a function of the hydrogeomorphological index of heavy-tailed flow behavior a. Red markers display the median values of a and b (squares), the interquartile intervals of b (vertical bars), and the binning ranges of a (horizontal bars, equal number of case studies in each bin), highlighting the correlation between the empirical power law exponent b and the hydrograph recession exponent a for confirmed heavy-tailed cases (black dots) in all three cases (i.e., daily streamflows, ordinary peak flows, and monthly flow maxima). We also test the correlation by calculating their distance correlation (Székely et al., 2007), which is valid for both potential linear and nonlinear associations between two random variables. We find that a and b are significantly correlated at a significance level of 0.05 in all three cases with distance (Spearman) correlation coefficients of 0.45, 0.44, and 0.81 (0.42, 0.46, and 0.60) for daily streamflows, ordinary peak flows, and monthly flow maxima. The last high value of correlation is likely affected by the existence of two clusters of black dots in Figure 2c. Nonetheless, the existence of a statistically significant correlation between the empirical power law exponent and the hydrogeomorphological index (confirmed for all panels a,b,c) confirms that the latter not only can be used to identify heavy-tailed flood behavior but also to evaluate the degree of the tail heaviness of the underlying distributions.

Figure 2c is of particular interest because it shows a common issue in the practice of flood hazard assessment. The power law is a plausible representation of the empirical distribution of monthly maxima in some cases (black dots) that are characterized by large values of the recession exponent a and are therefore classified as having heavy-tailed behavior according to the hydrogeomorphological index. In other cases (gray dots), conclusive evidence of possible heavy-tailed flood behavior cannot be drawn from the limited observations of monthly maxima. However, the hydrogeomorphological index retains its capability to provide estimates of the tail heaviness based on the value of the hydrograph recession exponent and classifies the case studies as heavy-tailed. Such a classification is deemed robust, provided that the predictions of the hydrogeomorhological index are confirmed by observations in cases (panels a and b) where data size is not a limitation (i.e., for daily streamflow and ordinary peak flows). The ability of the hydrogeomorphological index to infer the tail heaviness of flood distributions by examining the intrinsic dynamics of the hydrological system constitutes an advantage of the approach, that is especially useful in the very common cases when the tail of the flood distribution cannot be known from limited observations of maxima only.

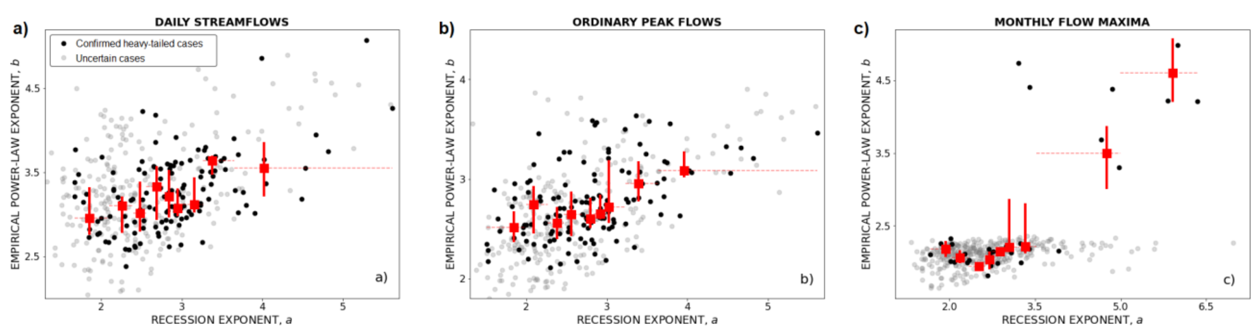

Figure 2. Empirical power law exponent b as a function of the hydrogeomorphological index of heavy-tailed behavior a. Case studies are classified into groups of confirmed heavy-tailed (black dots) and uncertain (gray dots) cases on the basis of the goodness-of-fit testing procedure (Clauset et al., 2009). The former denotes cases for which a power law provides a reliable description of the empirical data distribution, while the latter denotes cases whose data cannot convincingly support such a distribution. Red markers highlight the correlation between the empirical power law exponent b and the hydrograph recession exponent a for confirmed heavy-tailed cases in the case of (a) daily streamflows (n=121 case studies), (b) ordinary peak flows (n=116), and (c) monthly flow maxima (n=34). Red markers display the median values

of a and b (squares), the interquartile intervals of b (vertical bars), and the binning ranges of a (horizontal bars, equal number of case studies in each bin).

In Figure 3, we test the index stability of the categorization of case studies into heavy/nonheavy-tailed flood behavior for decreasing data lengths. We benchmark the hydrogeomorphological index (i.e., the hydrograph recession exponent a) against two other frequently used metrics of heavy tails in hydrological studies: (1) the upper tail ratio (UTR) (Lu et al., 2017; Smith et al., 2018; Villarini et al., 2011; Wang et al., 2022) and (2) the shape parameter ξ of the GEV distribution (Morrison & Smith, 2002; Papalexiou et al., 2013; Villarini & Smith, 2010). The UTR is derived as the ratio of the maximum record to the 0.9 quantiles of floods (Smith et al., 2018), and the ξ is estimated using the python package OpenTURNS 1.16 (Baudin et al., 2017). We compute both using data of monthly flow maxima. For all three indices ($a, UTR,$ and ξ), we estimate the index for decreasing data lengths from 35 (bounded by the shortest record length in the dataset) to 2 years in each case study. The index for each test length is calculated based on the median value of the estimates derived from 30 random fragments (with the assigned test length) of the entire record.

To have the reference of the stability of the categorization, we use the entire data record computing the values of the hydrogeomorphological index and the GEV shape parameter (notations with an asterisk in Figure 3, i.e., a^* and ξ^*). Each case study is categorized as either having (red) or not (green) the heavy-tailed behavior by the criteria of heavy (nonheavy) tails for the geomorphological index as $a^* > 2$ ($a^* < 2$) or for the GEV shape parameter as $\xi^* > 0$ ($\xi^* \leq 0$) (Godrèche et al., 2015). For the UTR, however, there is no specific threshold for the identification of heavy/nonheavy tails, but a larger value indicates a heavier tail.

The categorization of the hydrogeomorphological index is consistent across the test data length (Figure 3a). Specifically, the index estimates retain beyond 2 for most heavy-tailed cases (red) and below 2 for most nonheavy-tailed cases (green) when the data length decreases. The vertical shaded bar and line show the 0.25–0.75 and 0.05–0.95 quantile ranges of the index estimates across case studies. Besides the consistent categorization, the index estimates vary in a narrow range over the test data length both for the median value (i.e., from 2.64 to 2.92 for heavy-tailed cases and from 1.84 to 2.0 for nonheavy-tailed cases) and for the variation (e.g., the coefficient of variation ranges from 0.29 to 0.33 for heavy-tailed cases and from 0.29 to 0.33 for nonheavy-tailed cases). The small fluctuation of the variation across the test data length implies that the variation in index estimates is primarily caused by case study heterogeneity rather than decreasing data length. These results essentially confirm the stability of the hydrogeomorphological index for decreasing data lengths.

In contrast, the upper tail ratio shows pronounced instability for decreasing data lengths (Figure 3b). The median value of the index estimates ranges from 1.32 to 2.36, and the coefficient of variation ranges from 0.15 to 0.64, indicating that the tail heaviness is underestimated as data length decreases, in agreement with Smith et al. (2018) and Wietzke et al. (2020). The differential variation for decreasing data length denotes an apparent bias in the index estimates caused by the short data in addition to the heterogeneity across case studies.

Figure 3c shows the categorization of tail behavior based on the estimates of the GEV shape parameters. When the test data length is above five years, case studies with index estimates in the interquartile range (the vertical shaded bar) are consistent in the categorization of heavy/nonheavy-tailed behavior. When the data length is below five years, the underestimation of tail heaviness exists. Meanwhile, the index estimate changes slightly in its median but evidently in its coefficient of variation across the test data length. The former (latter) ranges from 0.39 to 0.52 (0.37 to 1.03) for the heavy-tailed cases and keeps 0 (--; the coefficient of variation is not applied for data with zero mean) for the nonheavy-tailed cases. These results show that the GEV shape parameter may still be considered a practical index for the heavy/nonheavy-tailed categorization because most applications have data that are more than five years. Nonetheless, the bias in the variation of index estimates across data length and the apparent underestimation in cases with very limited data point to the dependence on data lengths, in agreement with Papalexiou and Koutsoyiannis (2013).

We demonstrate the hydrogeomorphological index is robust in cases with limited data, i.e., it is stable in the categorization of heavy/nonheavy-tailed flood behavior for decreasing data lengths. Given that most data records worldwide are relatively short (Lins, 2008), this is a valuable tool to infer the tail behavior of streamflow in river basins. Moreover, given that generally all available records are too short of estimating the tail behavior of maxima (e.g., floods), this approach is even more valuable because it allows scientists or engineers to estimate the heavy-tailed flood behavior and assess the hazards from common discharge dynamics.

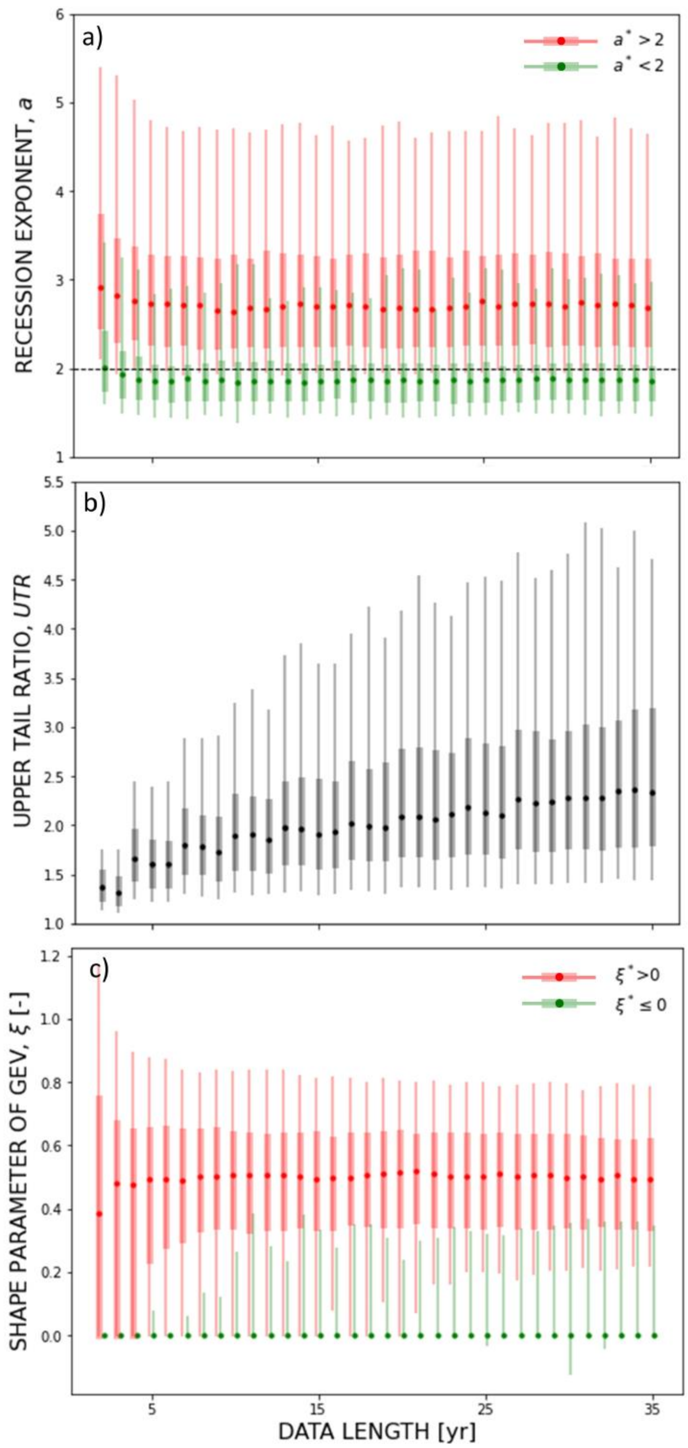

Figure 3. Stability of the categorization of case studies into heavy/nonheavy-tailed flood behavior for decreasing data lengths. Estimates of three different indices of tail behavior as a function of data length. (a) Hydrograph recession exponent a (i.e., the proposed hydrogeomorphological index of this study). Two frequently used metrics of heavy tails in hydrological studies: (b) the upper tail ratio UTR, and (c) the shape

parameter ξ of the GEV distribution. Dots display the median values of the estimates for 386 case studies; vertical shaded bars and lines respectively show the 0.25-0.75 and 0.05-0.95 quantile ranges of the estimates. The entire data record was used for computing the reference values of the hydrograph recession exponent α^* and the GEV shape parameter ξ^* and categorizing each case study as either having (red) or not (green) the heavy-tailed behavior.

5 Conclusions

The hydrograph recession exponent is identified as an index of heavy-tailed flood behavior from a physically-based description of hydrological dynamics. It is essentially a hydrogeomorphological index of heavy-tailed flood behavior because it originates from the geomorphological structure of the contributing river basin. We show that the proposed hydrogeomorphological index enables the identification of heavy/nonheavy-tailed flood behavior and the evaluation of the tail heaviness across case studies. Remarkably, it leverages the information of common discharge dynamics and shows robust identification of tail behavior for decreasing data length. We demonstrate all these capabilities in a large set of case studies across Germany on a seasonal basis, featuring the diversity in climatic and physiographic conditions. The hydrogeomorphological index addresses the limitations of other frequently used indices (e.g., lack of physical support, low effectiveness/ineffectiveness in cases with limited data) and allows for robust identification of heavy-tailed flood behavior, which is particularly useful in assessing hazards of extreme floods in data-scarce areas.

Acknowledgments

This work is funded by the Deutsche Forschungsgemeinschaft-Project 421396820 “Propensity of rivers to extreme floods: climate-landscape controls and early detection (PREDICTED)” and FOR 2416 “Space-Time Dynamics of Extreme Floods (SPATE)”. The financial support of the Helmholtz Centre for Environmental Research and the Norwegian Institute for Water Research is as well acknowledged. SY (the 3rd author) acknowledges the support of the Helmholtz Climate Initiative Project funded by the Helmholtz Association. The manuscript and supporting information provide all the information needed to replicate the results.

Data Availability Statement

For providing the discharge data for Germany, we are grateful to the Bavarian State Office of Environment (LfU, https://www.gkd.bayern.de/de/fluesse/abfluss) and the Global Runoff Data Centre (GRDC) prepared by the Federal Institute for Hydrology (BfG, http://www.bafg.de/GRDC). Climatic data can be obtained from the German Weather Service (DWD; ftp://ftp-cdc.dwd.de/pub/CDC/). The digital elevation model can be retrieved from Shuttle Radar Topography Mission (SRTM; https://cgiarcsi.community/data/srtm-90m-digital-elevation-database-v4-1/).

References

Arai, R., Toyoda, Y., & Kazama, S. (2020). Runoff recession features in an analytical probabilistic streamflow model. *Journal of Hydrology*, *597*, 125745. https://doi.org/10.1016/j.jhydrol.2020.125745

Basso, S., Botter, G., Merz, R., & Miniussi, A. (2021). PHEV! The PHysically-based Extreme Value distribution of river flows. *Environmental Research Letters*, *16*(12). https://doi.org/10.1088/1748-9326/ac3d59

Basso, S., Schirmer, M., & Botter, G. (2015). On the emergence of heavy-tailed streamflow distributions. *Advances in Water Resources*, *82*, 98–105. https://doi.org/10.1016/j.advwatres.2015.04.013

Basso, S., Schirmer, M., & Botter, G. (2016). A physically based analytical model of flood frequency curves. *Geophysical Research Letters*, *43*(17), 9070–9076. https://doi.org/10.1002/2016GL069915

Baudin, M., Dutfoy, A., Iooss, B., & Popelin, A.-L. (2017). OpenTURNS: An Industrial Software for Uncertainty Quantification in Simulation BT - Handbook of Uncertainty Quantification. In R. Ghanem, D. Higdon, & H. Owhadi (Eds.) (pp. 2001–2038). Cham: Springer International Publishing. https://doi.org/10.1007/978-3-319-12385-1_64

Beirlant, J., Goegebeur, Y., Teugels, J., Segers, J., De Waal, D., & Ferro, C. (2004). *Statistics of extremes: Theory and applications*. *Wiley*. https://doi.org/https://doi.org/10.1002/0470012382

Bernardara, P., Schertzer, D., Sauquet, E., Tchiguirinskaia, I., & Lang, M. (2008). The flood probability distribution tail: How heavy is it? *Stochastic Environmental Research and Risk Assessment*, *22*(1), 107–122. https://doi.org/10.1007/s00477-006-0101-2

Bevere, L., & Remondi, F. (2022). *Natural catastrophes in 2021: the floodgates are open*. *Swiss Re Institute sigma research*.

Biswal, B. (2021). Decorrelation is not dissociation: There is no means to entirely decouple the Brutsaert-Nieber parameters in streamflow recession analysis. *Advances in Water Resources*, *147*, 103822. https://doi.org/https://doi.org/10.1016/j.advwatres.2020.103822

Biswal, B., & Marani, M. (2010). Geomorphological origin of recession curves. *Geophysical Research Letters*, *37*(24), 1–5. https://doi.org/10.1029/2010GL045415

Biswal, B., & Marani, M. (2014). “Universal” recession curves and their geomorphological interpretation. *Advances in Water Resources*, *65*, 34–42. https://doi.org/10.1016/j.advwatres.2014.01.004

Biswal, B., & Nagesh Kumar, D. (2014). What mainly controls recession flows in river basins? *Advances in Water Resources*, *65*, 25–33. https://doi.org/10.1016/j.advwatres.2014.01.001

Botter, G., Basso, S., Porporato, A., Rodriguez-Iturbe, I., & Rinaldo, A. (2010). Natural streamflow regime alterations: Damming of the Piave river basin (Italy). *Water Resources Research*, *46*(6), 1–14. https://doi.org/10.1029/2009WR008523

Botter, G., Peratoner, F., Porporato, A., Rodriguez-Iturbe, I., & Rinaldo, A. (2007). Signatures of large-scale soil moisture dynamics on streamflow statistics across U.S. climate regimes. *Water Resources Research*, *43*(11), 1–10. https://doi.org/10.1029/2007WR006162

Botter, G., Porporato, A., Rodriguez-Iturbe, I., & Rinaldo, A. (2007). Basin-scale soil moisture dynamics and the probabilistic characterization of carrier hydrologic flows: Slow, leaching-prone components of the hydrologic response. *Water Resources Research*, *43*(2), 1–14. https://doi.org/10.1029/2006WR005043

Botter, G., Porporato, A., Rodriguez-Iturbe, I., & Rinaldo, A. (2009). Nonlinear storage-discharge relations and catchment streamflow regimes. *Water Resources Research*, *45*(10), 1–16. https://doi.org/10.1029/2008WR007658

Brutsaert, W., & Nieber, J. L. (1977). Regionalized drought flow hydrographs from a mature glaciated plateau. *Water Resources Research*, *13*(3), 637–643. https://doi.org/10.1029/WR013i003p00637

Ceola, S., Botter, G., Bertuzzo, E., Porporato, A., Rodriguez-Iturbe, I., & Rinaldo, A. (2010). Comparative study of ecohydrological streamflow probability distributions. *Water Resources Research*, *46*(9), 1–12. https://doi.org/10.1029/2010WR009102

Clauset, A., Shalizi, C. R., & Newman, M. E. J. (2009). Power-law distributions in empirical data. *SIAM Review*, *51*(4), 661–703. https://doi.org/10.1137/070710111

Cooke, R. M., Nieboer, D., & Misiewicz, J. (2014). *Fat-Tailed Distributions: Data, Diagnostics and Dependence* (volume 1). John Wiley & Sons.

Cooke, R. M., & Nieboer, D. (2011). Heavy-Tailed Distributions: Data, Diagnostics, and New Developments. *Resources for the Future Discussion Paper, No. 11-19*. https://doi.org/dx.doi.org/10.2139/ssrn.1811043

Doulatyari, B., Betterle, A., Basso, S., Biswal, B., Schirmer, M., & Botter, G. (2015). Predicting streamflow distributions and flow duration curves from landscape and climate. *Advances in Water Resources*, *83*, 285–298. https://doi.org/10.1016/j.advwatres.2015.06.013

Durrans, S. R., Eiffe, M. A., Thomas, W. O., & Goranflo, H. M. (2003). Joint Seasonal /Annual Flood Frequency Analysis. *Journal of Hydrologic Engineering*, *8*(4), 181–189. https://doi.org/10.1061/(asce)1084-0699(2003)8:4(181)

El Adlouni, S., Bobée, B., & Ouarda, T. B. M. J. (2008). On the tails of extreme event distributions in hydrology. *Journal of Hydrology*, *355*(1–4), 16–33. https://doi.org/10.1016/j.jhydrol.2008.02.011

Eliazar, I., & Sokolov, I. (2010). Gini characterization of extreme-value statistics. *Physica A-Statistical Mechanics and Its Applications - PHYSICA A*, *389*, 4462–4472. https://doi.org/10.1016/j.physa.2010.07.005

Else, H. (2021). Climate change implicated in Germany's deadly floods. *Nature*. https://doi.org/10.1038/d41586-021-02330-y

Embrechts, P., Klüppelberg, C., & Mikosch, T. (1997). *Modelling extreme events for insurance and finance*. Springer Berlin Heidelberg.

Fischer, S., & Schumann, A. (2016). Robust flood statistics: comparison of peak over threshold approaches based on monthly maxima and TL-moments. *Hydrological Sciences Journal*, *61*(3), 457–470. https://doi.org/10.1080/02626667.2015.1054391

Ghosh, D. K., Wang, D., & Zhu, T. (2016). On the transition of base flow recession from early stage to late stage. *Advances in Water Resources*, *88*, 8–13. https://doi.org/10.1016/j.advwatres.2015.11.015

Godrèche, C., Majumdar, S. N., & Schehr, G. (2015). Statistics of the longest interval in renewal processes. *Journal of Statistical Mechanics: Theory and Experiment*, *2015*(3). https://doi.org/10.1088/1742-5468/2015/03/P03014

Jachens, E. R., Rupp, D. E., Roques, C., & Selker, J. S. (2020). Recession analysis revisited: Impacts of climate on parameter estimation. *Hydrology and Earth System Sciences*, *24*(3), 1159–1170. https://doi.org/10.5194/hess-24-1159-2020

Katz, R. (2002). Statistics of Extremes in Climatology and Hydrology. *Advances in Water Resources*, *25*, 1287–1304.

Kondor, D., Pósfai, M., Csabai, I., & Vattay, G. (2014). Do the rich get richer? An empirical analysis of the Bitcoin transaction network. *PLoS ONE*, *9*(2). https://doi.org/10.1371/journal.pone.0086197

Laio, F., Porporato, A., Fernandez-Illescas, C. P., & Rodriguez-Iturbe, I. (2001). Plants in water-controlled ecosystems: Active role in hydrologic processes and responce to water stress IV. Discussion of real cases. *Advances in Water Resources*, *24*(7), 745–762. https://doi.org/10.1016/S0309-1708(01)00007-0

Lins, H. F. (2008). Challenges to hydrological observations. *WMO Bulletin*, *57*(January), 55–58.

Lu, P., Smith, J. A., & Lin, N. (2017). Spatial characterization of flood magnitudes over the drainage network of the Delaware river basin. *Journal of Hydrometeorology*, *18*(4), 957–976. https://doi.org/10.1175/JHM-D-16-0071.1

Malamud, B. D. (2004). Tails of natural hazards. *Physics World*, *17*(8), 31–35. https://doi.org/10.1088/2058-7058/17/8/35

Malamud, B. D., & Turcotte, D. L. (2006). The applicability of power-law frequency statistics to floods. *Journal of Hydrology*, *322*(1–4), 168–180. https://doi.org/10.1016/j.jhydrol.2005.02.032

McDermott, T. K. J. (2022). Global exposure to flood risk and poverty. *Nature Communications*, *13*(1), 6–8. https://doi.org/10.1038/s41467-022-30725-6

Mejía, A., Daly, E., Rossel, F., Javanovic, T., & Gironás, J. (2014). A stochastic model of streamflow for urbanized basins. *Water Resources Research*, *50*, 1984–2001. https://doi.org/10.1002/2013WR014834

Merz, B., Basso, S., Fischer, S., Lun, D., Blöschl, G., Merz, R., et al. (2022). Understanding heavy tails of flood peak distributions. *Water Resources Research*, 1–37. https://doi.org/10.1029/2021wr030506

Merz, B., Blöschl, G., Vorogushyn, S., Dottori, F., Aerts, J. C. J. H., Bates, P., et al. (2021). Causes, impacts and patterns of disastrous river floods. *Nature Reviews Earth and Environment*, *2*(9), 592–609. https://doi.org/10.1038/s43017-021-00195-3

Merz, R., & Blöschl, G. (2009). Process controls on the statistical flood moments - a data based analysis. *Hydrological Processes*, *23*(5), 675–696. https://doi.org/10.1002/hyp

Morrison, J. E., & Smith, J. A. (2002). Stochastic modeling of flood peaks using the generalized extreme value distribution. *Water Resources Research*, *38*(12), 41-1-41–12. https://doi.org/10.1029/2001wr000502

Müller, M. F., Dralle, D. N., & Thompson, S. E. (2014). Analytical model for flow duration curves in seasonally dry climates. *Water Resources Research*, *50*, 5510–5531. https://doi.org/10.1002/2014WR015301

Müller, M. F., Roche, K. R., & Dralle, D. N. (2021). Catchment processes can amplify the effect of increasing rainfall variability. *Environmental Research Letters*, *16*(8). https://doi.org/10.1088/1748-9326/ac153e

Mutzner, R., Bertuzzo, E., Tarolli, P., Weijs, S. V., Nicotina, L., Ceola, S., et al. (2013). Geomorphic signatures on Brutsaert base flow recession analysis. *Water Resources Research*, *49*(9), 5462–5472. https://doi.org/10.1002/wrcr.20417

Nerantzaki, S. D., & Papalexiou, S. M. (2019). Tails of extremes: Advancing a graphical method and harnessing big data to assess precipitation extremes. *Advances in Water Resources*, *134*. https://doi.org/10.1016/j.advwatres.2019.103448

Papalexiou, S. M., Koutsoyiannis, D., & Makropoulos, C. (2013). How extreme is extreme? An assessment of daily rainfall distribution tails. *Hydrology and Earth System Sciences*, *17*(2), 851–862. https://doi.org/10.5194/hess-17-851-2013

Papalexiou, S. M., & Koutsoyiannis, D. (2013). Battle of extreme value distributions : A global survey on extreme daily rainfall. *Water Resources Research*, *49*(1), 187–201. https://doi.org/10.1029/2012WR012557

Porporato, A., Daly, E., & Rodriguez-Iturbe, I. (2004). Soil water balance and ecosystem response to climate change. *American Naturalist*, *164*(5), 625–632. https://doi.org/10.1086/424970

Pumo, D., Viola, F., La Loggia, G., & Noto, L. V. (2014). Annual flow duration curves assessment in ephemeral small basins. *Journal of Hydrology*, *519*(PA), 258–270. https://doi.org/10.1016/j.jhydrol.2014.07.024

Rajah, K., O'Leary, T., Turner, A., Petrakis, G., Leonard, M., & Westra, S. (2014). Changes to the temporal distribution of daily precipitation. *Geophysical Research Letters*, *41*(24), 8887–8894. https://doi.org/10.1002/2014GL062156

Rentschler, J., Salhab, M., & Jafino, B. A. (2022). Flood exposure and poverty in 188 countries. *Nature Communications*, *13*(1), 3527. https://doi.org/10.1038/s41467-022-30727-4

Resnick, S. I. (2007). *Heavy-Tail Phenomena: Probabilistic and Statistical Modeling*. New York: Springer US.

Santos, A. C., Portela, M. M., Rinaldo, A., & Schaefli, B. (2018). Analytical flow duration curves for summer streamflow in Switzerland. *Hydrology and Earth System Sciences*, *22*(4), 2377–2389. https://doi.org/10.5194/hess-22-2377-2018

Sartori, M., & Schiavo, S. (2015). Connected we stand: A network perspective on trade and global food security. *Food Policy*, *57*, 114–127. https://doi.org/https://doi.org/10.1016/j.foodpol.2015.10.004

Schaefli, B., Rinaldo, A., & Botter, G. (2013). Analytic probability distributions for snow-dominated streamflow. *Water Resources Research*, *49*(5), 2701–2713. https://doi.org/10.1002/wrcr.20234

Smith, J. A., Cox, A. A., Baeck, M. L., Yang, L., & Bates, P. (2018). Strange Floods: The Upper Tail of Flood Peaks in the United States. *Water Resources Research*, *54*(9), 6510–6542. https://doi.org/10.1029/2018WR022539

Székely, G. J., Rizzo, M. L., & Bakirov, N. K. (2007). Measuring and testing dependence by correlation of distances. *Annals of Statistics*, *35*(6), 2769–2794. https://doi.org/10.1214/009053607000000505

Tarasova, L., Basso, S., & Merz, R. (2020). Transformation of Generation Processes From Small Runoff Events to Large Floods. *Geophysical Research Letters*, *47*(22). https://doi.org/10.1029/2020GL090547

Tashie, A., Pavelsky, T., & Band, L. E. (2020). An Empirical Reevaluation of Streamflow Recession Analysis at the Continental Scale. *Water Resources Research*, *56*(1), 1–18. https://doi.org/10.1029/2019WR025448

Tashie, A., Pavelsky, T., & Emanuel, R. E. (2020). Spatial and Temporal Patterns in Baseflow Recession in the Continental United States. *Water Resources Research*, *56*(3), 1–18. https://doi.org/10.1029/2019WR026425

Tashie, A., Scaife, C. I., & Band, L. E. (2019). Transpiration and subsurface controls of streamflow recession characteristics. *Hydrological Processes*, *33*(19), 2561–2575. https://doi.org/10.1002/hyp.13530

Vázquez, A., Oliveira, J. G., Dezsö, Z., Goh, K. Il, Kondor, I., & Barabási, A. L. (2006). Modeling bursts and heavy tails in human dynamics. *Physical Review E - Statistical, Nonlinear, and Soft Matter Physics*, *73*(3), 1–19. https://doi.org/10.1103/PhysRevE.73.036127

Villarini, G., & Smith, J. A. (2010). Flood peak distributions for the eastern United States. *Water Resources Research*, *46*(6), 1–17. https://doi.org/10.1029/2009WR008395

Villarini, G., Smith, J. A., Baeck, M. L., Marchok, T., & Vecchi, G. A. (2011). Characterization of rainfall distribution and flooding associated with U.S. landfalling tropical cyclones: Analyses of Hurricanes Frances, Ivan, and Jeanne (2004). *Journal of Geophysical Research Atmospheres*, *116*(23). https://doi.org/10.1029/2011JD016175

Wang, H., Merz, R., Yang, S., Tarasova, L., & Basso, S. (2022). Emergence of heavy tails in streamflow distributions: the role of spatial rainfall variability. *Advances in Water Resources Journal*, *171*(104359). https://doi.org/10.1016/j.advwatres.2022.104359

Wietzke, L. M., Merz, B., Gerlitz, L., Kreibich, H., Guse, B., Castellarin, A., & Vorogushyn, S. (2020). Comparative analysis of scalar upper tail indicators. *Hydrological Sciences Journal*, *65*(10), 1625–1639. https://doi.org/10.1080/02626667.2020.1769104

Zorzetto, E., Botter, G., & Marani, M. (2016). On the emergence of rainfall extremes from ordinary events. *Geophysical Research Letters*, *43*(15), 8076–8082. https://doi.org/10.1002/2016GL069445

Geophysical Research Letters

Supporting Information for

A hydrogeomorphological index of heavy-tailed flood behavior

H. -J. Wang[1], R. Merz[1,2], S. Yang[3], and S. Basso[1,4]

[1]Department of Catchment Hydrology, Helmholtz Centre for Environmental Research – UFZ, Halle (Saale), Germany,

[2]Institute of Geosciences and Geography, Martin-Luther University Halle-Wittenberg, Halle (Saale), Germany,

[3]Department of Aquatic Ecosystem Analysis, Helmholtz Centre for Environmental Research – UFZ, Magdeburg, Germany

[4]Norwegian Institute for Water Research (NIVA), Oslo, Norway

Contents of this file

Introduction

This supporting information contains two supplementary methods and one figure. Text S1 is the theory of identifying tail behavior for distributions of peak flows and flow maxima from hydrological dynamics. Text S2 is the method we used to test the power law hypothesis. Figure S1 is a reference map of the analyzed basins.

Text S1. Identifying tail behavior for distributions of peak flows and flow maxima from hydrological dynamics

The probability distribution of ordinary peak flows (i.e., local flow peaks generated by streamflow-producing rainfall events (Zorzetto et al., 2016)) and flow maxima (i.e. maximum values in a specified time frame) can be analytically expressed as $p_j(q)$ and $p_M(q)$, respectively (Basso et al., 2016):

$$p_j(q) = C_2 \cdot q^{1-a} \cdot e^{-\frac{q^{2-a}}{\alpha K(2-a)}} \cdot e^{\frac{q^{1-a}}{K(1-a)}} \tag{S1}$$

$$p_M(q) = p_j(q) \cdot \lambda\tau \cdot e^{-\lambda\tau \cdot D_j(q)}, \qquad D_j(q) = \int_q^\infty p_j(q)\, dq \tag{S2}$$

where $\tau[day]$ is the duration of the specified time frame, C_2 is normalization constants, and all the other notations have been listed in the main context.

To analyze the tail behavior of these distributions, we take the limit of $q \longrightarrow +\infty$ for both Equations S1 and S2. Because $\lim_{q\to\infty} D_j(q) = \int_\infty^\infty p_j(q)\, dq = 0$, the Equations S1 and S2 can be transformed into: (set $C_3 = \lambda\tau C_2$)

$$\lim_{q\to\infty} p_j(q) = \begin{cases} C_2 \cdot q^{1-a} \cdot e^{-\frac{q^{2-a}}{\alpha K(2-a)}}, & 1 < a < 2 \\ C_2 \cdot q^{1-a}, & a > 2 \end{cases} \tag{S3}$$

$$\lim_{q\to\infty} p_M(q) = \begin{cases} C_3 \cdot q^{1-a} \cdot e^{-\frac{q^{2-a}}{\alpha K(2-a)}}, & 1 < a < 2 \\ C_3 \cdot q^{1-a}, & a > 2 \end{cases} \tag{S4}$$

For both of the cases, the tail behavior is determined by a power law term and an exponential term when $1 < a < 2$, which indicates the tail decreases slower than the exponential but faster than the power law tail; while the tail behavior is solely determined by a power law function, representing heavy-tailed flow distribution when a > 2. Therefore, the hydrograph recession exponent ($a > 2$) is shown as an indicator of the heavy-tailed flood behavior.

Text S2. Testing the power law hypothesis

Every empirical data distribution can be fitted by a power law model no matter what is the true distribution from which the data is drawn. To identify case studies for which the power law is a plausible distribution of the observed data, we test the power law hypothesis by means of the method of Clauset et al. (2009), which statistically confirms whether the power law distribution fitted on the empirical data provides a reliable description of those data. We compute this goodness-of-fit framework via the function test_pl in the python package plfit 1.0.3 (https://pypi.org/project/plfit/).

The challenge here is to discern the errors caused by the sampling randomness from those arising because the data might be actually drawn from another distribution rather than the power law. The principle of the approach is to first measure the error distance ε_d between the empirical data and the optimized power law model, which is the distance need to be tested. Secondly, we generate a number of synthetic data samples by randomly sampling from the optimized power law model. The error distance ε_s between the synthetic data and the optimized power law model is measured, indicating the fluctuation caused by randomness only. A power law hypothesis is accepted if $\varepsilon_d < \varepsilon_s$ but rejected if $\varepsilon_d > \varepsilon_s$.

However, it is possible that non-power-law empirical data also has a smaller ε_d than ε_s. To address this issue, a great number n of iterations via the Monte-Carlo test for this approach is needed.

The Kolmogorov-Smirnov statistic is used to measure the error distance with $n = 1000$ (as suggested by Clauset et al. (2009)). In the meanwhile, the p-value is defined as the frequency of $\varepsilon_s > \varepsilon_d$. The power law hypothesis is ruled out if $p \leq 0.1$ whereas it is confirmed as plausible if $p > 0.1$. We, therefore, term all the qualified cases (i.e., $p > 0.1$) ‘confirmed heavy-tailed cases’ to indicate their empirical power law distributions are convincingly supported by the data, whereas the others are not.

It is worth mentioning that, statistically, we cannot say those who does not qualify ‘are not’ power law distributions. There are at least two potential reasons for this result: (1) they are indeed not power law functions, or (2) The empirical data do not represent well the actual underlying distribution, often due to small sample sizes.

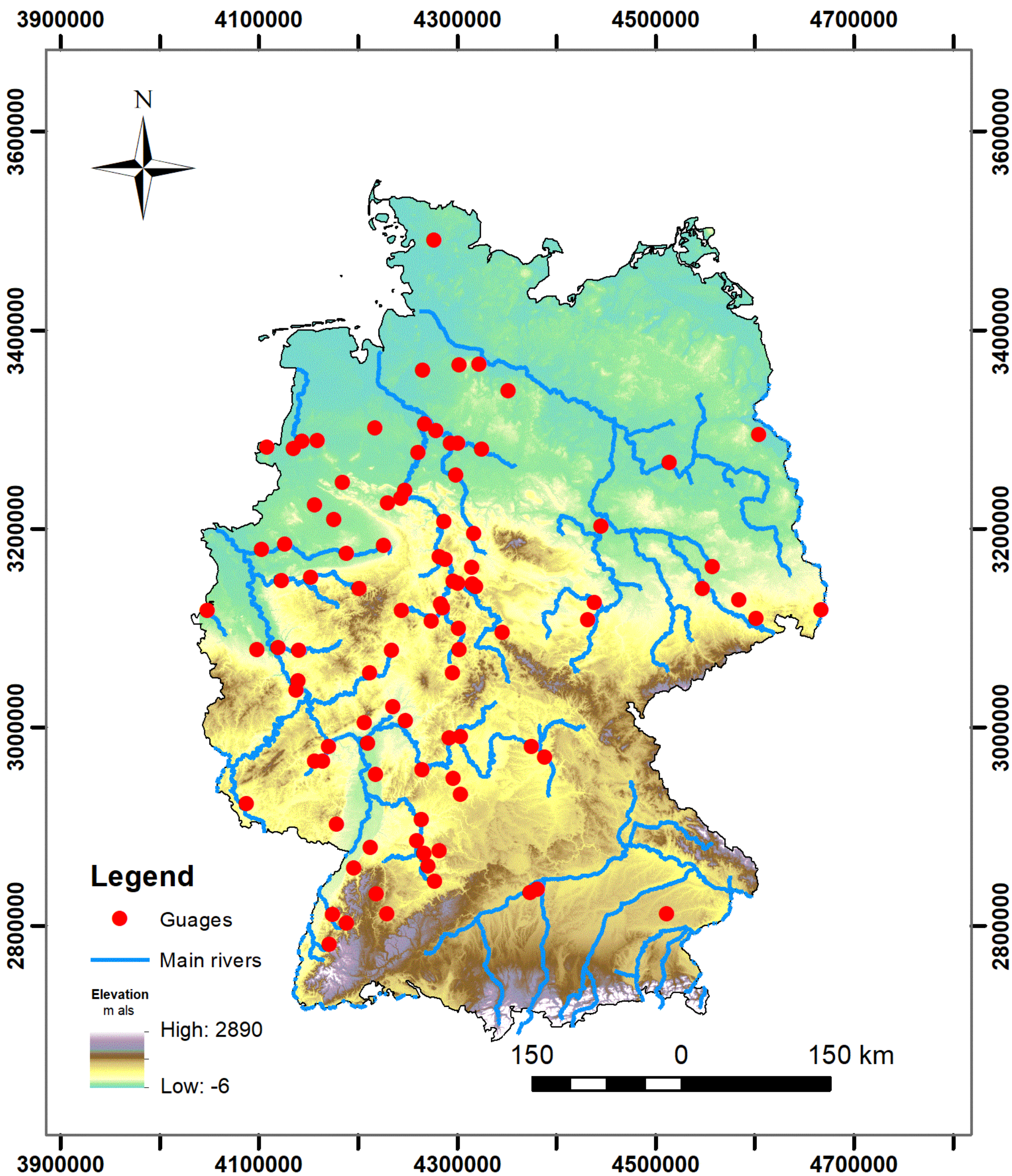

Figure S1. A reference map of 98 streamflow gauges across Germany. These river basins encompass a variety of climate and physiographic settings, without strong impact from snow dynamics. Their areas range from 110 to 23,843 km^2 with a median value of 1,195 km^2. The minimum, median, and maximum lengths of the daily streamflow records are 35, 58, and 63 years (inbetween 1951 – 2013).